Fuchs, A., Cella, M., Kondo, T., Colonna, M., 2005. Paradoxic inhibition of human natural interferon-producing cells by the activating receptor NKp44. Blood 106, 2076–2082.

Gays, F., Aust, J.G., Reid, D.M., Falconer, J., Toyama-Sorimachi, N., Taylor, P.R., Brooks, C.G., 2006. Ly49B is expressed on multiple subpopulations of myeloid cells. J. Immunol. 177, 5840–5851.

Hamerman, J.A., Jarjoura, J.R., Humphrey, M.B., Nakamura, M.C., Seaman, W.E., Lanier, L.L., 2006. Cutting edge: inhibition of TLR and FcR responses in macrophages by triggering receptor expressed on myeloid cells (TREM)-2 and DAP12. J. Immunol. 177, 2051–2055.

Hanke, T., Takizawa, H., McMahon, C.W., Busch, D.H., Pamer, E.G., Miller, J.D., Altman, J.D., Liu, Y., Cado, D., Lemonnier, F.A., Bjorkman, P.J., Raulet, D.H., 1999. Direct assessment of MHC class I binding by seven Ly49 inhibitory NK cell receptors. Immunity 11, 67–77.

Hao, L., Nei, M., 2004. Genomic organization and evolutionary analysis of Ly49 genes encoding the rodent natural killer cell receptors: rapid evolution by repeated gene duplication. Immunogenetics 56, 343–354.

Kamogawa-Schifter, Y., Ohkawa, J., Namiki, S., Arai, N., Arai, K., Liu, Y., 2005. Ly49Q defines 2 pDC subsets in mice. Blood 105, 2787–2792.

Kim, S., Poursine-Laurent, J., Truscott, S.M., Lybarger, L., Song, Y.J., Yang, L., French, A.R., Sunwoo, J.B., Lemieux, S., Hansen, T.H., Yokoyama, W.M., 2005. Licensing of natural killer cells by host major histocompatibility complex class I molecules. Nature 436, 709–713.

Krug, A., French, A.R., Barchet, W., Fischer, J.A., Dzionek, A., Pingel, J.T., Orihuela, M.M., Akira, S., Yokoyama, W.M., Colonna, M., 2004. TLR9-dependent recognition of MCMV by IPC and DC generates coordinated cytokine responses that activate antiviral NK cell function. Immunity 21, 107–119.

Kumanovics, A., Madan, A., Qin, S., Rowen, L., Hood, L., Fischer, L.K., 2002. Quod erat faciendum: sequence analysis of the H2-D and H2-Q regions of 129/SvJ mice. Immunogenetics 54, 479–489.

Liu, Y.J., 2005. IPC: professional type 1 interferon-producing cells and plasmacytoid dendritic cell precursors. Annu. Rev. Immunol. 23, 275–306.

Makrigiannis, A.P., Patel, D., Goulet, M.L., Dewar, K., Anderson, S.K., 2005. Direct sequence comparison of two divergent class I MHC natural killer cell receptor haplotypes. Genes Immun. 6, 71–83.

Makrigiannis, A.P., Pau, A.T., Saleh, A., Winkler-Pickett, R., Ortaldo, J.R., Anderson, S.K., 2001. Class I MHC-binding characteristics of the 129/J Ly49 repertoire. J. Immunol. 166, 5034–5043.

Nakano, H., Yanagita, M., Gunn, M.D., 2001. CD11c(+)B220(+)Gr-1(+) cells in mouse lymph nodes and spleen display characteristics of plasmacytoid dendritic cells. J. Exp. Med. 194, 1171–1178.

Naper, C., Dai, K.Z., Kveberg, L., Rolstad, B., Niemi, E.C., Vaage, J.T., Ryan, J.C., 2005. Two structurally related rat Ly49 receptors with opposing functions (Ly49 stimulatory receptor 5 and Ly49 inhibitory receptor 5) recognize nonclassical MHC class Ib-encoded target ligands. J. Immunol. 174, 2702–2711.

Nylenna, O., Naper, C., Vaage, J.T., Woon, P.Y., Gauguier, D., Dissen, E., Ryan, J.C., Fossum, S., 2005. The genes and gene organization of the Ly49 region of the rat natural killer cell gene complex. Eur. J. Immunol. 35, 261–272.

Omatsu, Y., Iyoda, T., Kimura, Y., Maki, A., Ishimori, M., Toyama-Sorimachi, N., Inaba, K., 2005. Development of murine plasmacytoid dendritic cells defined by increased expression of an inhibitory NK receptor, Ly49Q. J. Immunol. 174, 6657–6662.

Powis, S.J., Townsend, A.R., Deverson, E.V., Bastin, J., Butcher, G.W., Howard, J.C., 1991. Restoration of antigen presentation to the mutant cell line RMA-S by an MHC-linked transporter. Nature 354, 528–531.

Proteau, M.-F., Rousselle, E., Makrigiannis, A.P., 2004. Mapping of the BALB/c Ly49 cluster defines a minimal natural killer cell receptor gene repertoire. Genomics 84, 669–677.

Salio, M., Palmowski, M.J., Atzberger, A., Hermans, I.F., Cerundolo, V., 2004. CpG-matured murine plasmacytoid dendritic cells are capable of in vivo priming of functional CD8 T cell responses to endogenous but not exogenous antigens. J. Exp. Med. 199, 567–579.

Sanderson, S., Shastri, N., 1994. LacZ inducible, antigen/MHC-specific T cell hybrids. Int. Immunol. 6, 369–376.

Su, R.C., Kung, S.K., Silver, E.T., Lemieux, S., Kane, K.P., Miller, R.G., 1999. Ly-49CB6 NK inhibitory receptor recognizes peptide-receptive H-2Kb. J. Immunol. 163, 5319–5330.

Tabeta, K., Georgel, P., Janssen, E., Du, X., Hoebe, K., Crozat, K., Mudd, S., Shamel, L., Sovath, S., Goode, J., Alexopoulou, L., Flavell, R.A., Beutler, B., 2004. Toll-like receptors 9 and 3 as essential components of innate immune defense against mouse cytomegalovirus infection. Proc. Natl. Acad. Sci. U.S.A. 101, 3516–3521.

Toyama-Sorimachi, N., Omatsu, Y., Onoda, A., Tsujimura, Y., Iyoda, T., Kikuchi-Maki, A., Sorimachi, H., Dohi, T., Taki, S., Inaba, K., Karasuyama, H., 2005. Inhibitory NK receptor Ly49Q is expressed on subsets of dendritic cells in a cellular maturation- and cytokine stimulation-dependent manner. J. Immunol. 174, 4621–4629.

Toyama-Sorimachi, N., Tsujimura, Y., Maruya, M., Onoda, A., Kubota, T., Koyasu, S., Inaba, K., Karasuyama, H., 2004. Ly49Q, a member of the Ly49 family that is selectively expressed on myeloid lineage cells and involved in regulation of cytoskeletal architecture. Proc. Natl. Acad. Sci. U.S.A. 101, 1016–1021.

Wilhelm, B.T., Mager, D.L., 2004. Rapid expansion of the Ly49 gene cluster in rat. Genomics 84, 218–221.

Dose-Dependent Differential Regulation of Cytokine Secretion from Macrophages by Fractalkine[1]

Noriko Mizutani,* Toshiharu Sakurai,† Takahiro Shibata,‡ Koji Uchida,‡ Jun Fujita,† Rei Kawashima,* Yuki I. Kawamura,*§ Noriko Toyama-Sorimachi,* Toshio Imai,¶ and Taeko Dohi[2]*§

Although expression of the fractalkine (CX3CL1, FKN) is enhanced in inflamed tissues, it is detected at steady state in various organs such as the intestine, and its receptor CX3CR1 is highly expressed in resident-type dendritic cells and macrophages. We hypothesized that FKN might regulate the inflammatory responses of these cells. Therefore, murine macrophages were pretreated with FKN and then stimulated with LPS. We found that macrophages pretreated with 0.03 nM FKN but not with 3 nM FKN secreted 50% less TNF-α than did cells treated with LPS alone. Cells treated with 0.03 nM FKN and LPS also showed reduced phosphorylation of ERK1/2 and reduced NF-κB p50 subunit. Interestingly, the p65 subunit of NF-κB was translocated to the nuclei but redistributed to the cytoplasm in the early phase by forming a complex with peroxisome proliferator-activated receptor (PPAR) γ. Exogenous 15-deoxy-Δ(12,14)-prostaglandin J2, a natural ligand for PPAR-γ, also induced redistribution of p65 with decreased TNF-α secretion after LPS challenge. Pretreatment with 0.03 nM but not 3 nM FKN increased the cellular levels of 15-deoxy-Δ(12,14)-prostaglandin J2 as well as mRNA of PPAR-γ. Requirement of PPAR-γ for the effect of 0.03 nM FKN was confirmed by small interfering RNA of PPAR-γ. In contrast, pretreatment with 3 nM FKN induced higher levels of IL-23 compared with cells pretreated with 0.03 nM FKN and produced TNF-α in a CX3CR1-dependent manner. These dose-dependent differential effects of FKN establish its novel role in immune homeostasis and inflammation. ***The Journal of Immunology*****, 2007, 179: 7478–7487.**

Fractalkine (CX3CL1, FKN[3]) is a unique chemokine produced as a membrane-bound molecule that consists of an intracellular tail, a short membrane-spanning region, and a glycosylated mucin-like stalk that extends from the cell surface holding the chemokine domain (1). FKN also exists as a soluble glycoprotein that is produced by proteolytic cleavage of the full-length molecule at a membrane-proximal site (2, 3). Expression of FKN in endothelial cells is induced by various inflammatory stimuli such as LPS, TNF-α, IL-1, and IFN-γ (4–6). Besides induction of chemotaxis, FKN also functions as an adhesion molecule to support leukocyte adhesion and transmigration (7, 8). A unique receptor for FKN, CX3CR1, is expressed abundantly by dendritic cells and macrophages/monocytes (9–11) as well as Th-type 1 cells, cytotoxic effector lymphocytes (12, 13), mast cells (14), neurons, astrocytes, and microglia (15–17). Since expression of FKN and expression of CX3CR1 can be induced by immune cells, studies have focused on the role of FKN as an inflammatory mediator. Indeed, FKN is up-regulated in the inflammatory site of rheumatoid arthritis (12, 18), inflammatory bowel disease (19), atherosclerosis (20), psoriasis (21), myositis (22), and various inflammatory conditions of the kidney (23) and brain (24), although FKN gene-disrupted mice did not show significant differences from wild-type mice in either steady-state or inflammatory conditions (25).

Conversely, studies using GFP/CX3CR1 knock-in mice have shown that a $CX3CR1^{high}CCR2^{-}Gr1^{-}$ subset of murine blood monocytes characterized by CX3CR1-dependent recruitment to noninflamed tissues and a short-lived $CX3CR1^{low}CCR2^{+}Gr1^{+}$ cell population is actively recruited to inflamed tissue (26). Furthermore, CX3CR1-positive dendritic cells are distributed abundantly in the lamina propria of the normal intestine (27). Recent studies have shown that circulating $CX3CR1^{+}CD117Lin^{-}$ precursors represent the origin of some subsets of resident macrophages and dendritic cells (28), and a small proportion of intestinal lymph dendritic cells are derived from $CX3CR1^{high}$ blood monocytes in vivo under steady-state conditions (29). These results indicated the role of the FKN/CX3CR1 system in homing of noninflammatory or resident subsets of dendritic cells and macrophages. Of interest, a considerable amount of FKN is produced by epithelial cells and other types of cells in the normal intestine (19, 30). In addition to its role in cell dynamics, we assumed that the physiological level of FKN in the intestine regulates the function of $CX3CR1^{+}$ macrophages. Resident macrophages in the normal intestine have the distinctive feature of hyporesponsiveness to various inflammatory stimuli, including bacterial components (31–33). This is in sharp contrast to circulating monocytes and splenic macrophages, which

*Department of Gastroenterology, Research Institute, International Medical Center of Japan, Tokyo, Japan; †Department of Clinical Molecular Biology, Faculty of Medicine, Kyoto University, Kyoto, Japan; ‡Laboratory of Food and Biodynamics, Graduate School of Bioagricultural Sciences, Nagoya University, Nagoya, Japan; and §Core Research for Engineering, Science, and Technology and ¶KAN Research Institute Inc., Kobe, Japan

Received for publication January 9, 2007. Accepted for publication September 25, 2007.

The costs of publication of this article were defrayed in part by the payment of page charges. This article must therefore be hereby marked *advertisement* in accordance with 18 U.S.C. Section 1734 solely to indicate this fact.

[1] This work was supported in part by grants and contracts from the Ministry of Health, Labour and Welfare, the Ministry of Education, Culture, Sports, Science and Technology, the Japan Health Sciences Foundation, Novartis Foundation (Japan) for the Promotion of Science, and the Mitsukoshi Health and Welfare Foundation.

[2] Address correspondence and reprint requests to Dr. Taeko Dohi, Department of Gastroenterology, Research Institute, International Medical Center of Japan, Toyama 1-21-1, Shinjuku, Tokyo, Japan. E-mail address: dohi@ri.imcj.go.jp

[3] Abbreviations used in this paper: FKN, fractalkine (CX3CL1); BMϕ, bone marrow-derived macrophage; 15d-PGJ_2, 15-deoxy-$\Delta^{12,14}$-prostaglandin J2; PPAR-γ, peroxisome proliferator-activated receptor γ; siRNA, small interfering RNA.

produce large amounts of proinflammatory cytokines in response to bacterial components. The inflammatory anergy of intestinal macrophages is thought to be important to maintain intestinal homeostasis. However, the mechanism by which macrophages acquire this feature is not yet fully understood. One important working hypothesis is that intestinal epithelial cells and stromal cells provide a particular microenvironment to promote inflammatory anergy, along with a variety of cytokines and chemokines as their products. Indeed, intestinal stromal cell-derived products down-regulate both monocyte receptor expression and cytokine production (32). It is also likely that FKN participates in forming this microenvironment of the intestine to render macrophages immunologically hyporesponsive. Such anti-inflammatory activity of FKN has been reported previously. For example, FKN attenuated LPS-induced production of NO, IL-6, and TNF-α by rat (34) and mouse (17) microglia, which are phagocytotic cells and are responsible for cytokine production in the CNS. Pretreatment of rats with an anti-FKN Ab enhanced LPS-induced TNF-α levels in hippocampus and cerebrospinal fluid (35). However, the anti-inflammatory effect of FKN in bone marrow-derived or blood macrophages has not been documented.

In this study, we compared the effects of different concentrations of FKN on macrophages and found that relatively low concentrations of FKN suppressed LPS-induced TNF-α secretion by both bone marrow-derived macrophages (BMϕ) and the mouse macrophage cell line RAW264.7. We investigated the underlying mechanism and found for the first time that FKN induced the expression of both peroxisome proliferator-activated receptor (PPAR) γ and its ligand and altered the subunit usage of NF-κB after stimulation with LPS in macrophages, eventually decreasing the secretion of TNF-α. In contrast, higher concentrations of FKN, which may represent a local inflammatory condition, did not show such an immunosuppressive effect; instead, an up-regulation of IL-23 was seen.

Materials and Methods

Mice

Six- to 7-wk-old male C57BL/6J mice obtained from CLEA Japan and IL-10 knockout mice (C57BL/6J background; The Jackson Laboratory) were maintained under pathogen-free conditions in a facility of the Research Institute, International Medical Center of Japan (Tokyo, Japan). All experiments were performed according to the Institutional Guidelines for the Care and Use of Laboratory Animals in Research with the approval of the local ethics committee in the International Medical Center of Japan.

Histological immunostaining

Frozen sections were prepared from mouse intestine, fixed with cold acetone for 10 min, dried, and treated with Blockace (Dainippon Pharmaceuticals), incubated with hamster anti-FKN (22) or PE-labeled rat anti-F4/80 (Serotec) and rabbit anti-CX3CR1 (22), followed by secondary FITC-labeled anti-hamster IgG Ab (Southern Biotechnology Associates) or Alexa 488-labeled anti-rabbit IgG Ab (Invitrogen Life Technologies and Molecular Probes). Images were captured with a fluorescence microscope (BX50/BXFLA; Olympus) equipped with a CCD camera. Merged images were produced using Adobe Photoshop CS2 (Adobe Systems).

Cell culture, pretreatment with FKN, and stimulation with LPS

To obtain BMϕ, bone marrow cells were harvested and differentiated in DMEM containing 10 ng/ml M-CSF and 10% FBS for 7 days. RAW264.7 cells (American Type Culture Collection) were grown in DMEM supplemented with 10% FCS. Aliquots of 1×10^5 cells in 0.2 ml of culture medium were pretreated with the indicated concentration of recombinant mouse FKN (R&D Systems) for 12 h and then stimulated by addition of the indicated concentration of LPS (from *Salmonella minnesota*, L-2167; Sigma-Aldrich) to the culture. In some experiments, 15d-PGJ2 (Cayman Chemical) and mouse rIL-23 (R&D Systems) was added to the culture. To examine the effect of immobilized FKN, 96-well flat-bottom plates were coated with 0.1 ml of various concentrations of FKN in PBS for 12 h at 4°C. After washing with PBS, cells were placed and the culture was performed as above. Actual density of coated FKN after washing was not measured. The hamster anti-mouse FKN Ab for blocking FKN was prepared at KAN Research Institute (Kobe, Japan). To neutralize the effects of CX3CR1, purified rabbit anti-rat CX3CR1 polyclonal Ab (2 μg/ml; Torrey Pines Biolabs) was used with rabbit IgG (IBL) as a control. To neutralize the actions of IL-23, purified rat anti-mouse IL-23 p19 mAb (2 μg/ml; eBioscience) and purified rat IgG1 isotype control (BD Biosciences) were used as controls.

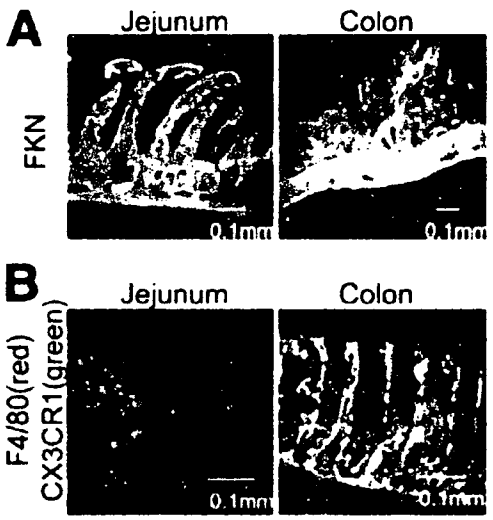

FIGURE 1. Expression of FKN in the intestine and detection of CX3CR1-positive macrophages. *A*, Frozen intestinal sections were stained with anti-FKN Ab. *B*, Frozen sections were double stained with anti-F4/80 (red) and anti-CX3CR1 Ab (green). Merged images are shown.

Cytokine production assay by ELISA

The concentrations of cytokines in culture supernatants were measured using a Murine TNF-α ELISA Development Kit (PeproTech), Quantikine M Mouse IL-6 Immunoassay kit (R&D Systems) and Mouse IL-10 ELISA kit (Endogen).

Flow cytometry analysis

Cells were incubated with mAb against mouse TLR4/MD-2 complex (SA15-21; a gift from Dr. S. Takamura-Akashi, Tokyo University, Tokyo, Japan) or isotype control IgG directly conjugated with Alexa 488 and analyzed by FACS (BD Biosciences).

Western blotting and immunoprecipitation

Cells were lysed in a buffer containing 150 mM NaCl, 50 mM Tris-Cl, 1 mM EDTA, 1 mM Na_3VO_4, 1 mM PMSF, 1% Nonidet P-40, complete protease inhibitor mixture (Roche Molecular Biochemicals), and 50 mM NaF (pH 8.0) for 20 min on ice. After centrifugation at $10,000 \times g$ for 20 min, protein concentrations were determined using the Bio-Rad protein assay. After separation by SDS-PAGE under reducing conditions, lysates were transferred to membranes (Immobilon; Millipore) and subsequently immunoblotted with specific Ab before visualization by chemiluminescence (SuperSignal West Dura; Pierce). To analyze ERK1/2 activation, membranes were probed with anti-phospho ERK 1/2 Ab or total ERK1/2 Ab (Cell Signaling Technology) and then stripped and reprobed with Ab to actin (Santa Cruz Biotechnology). To detect the amount of NF-κB p50 protein, nuclear extracts were subjected to Western blotting with anti-NF-κB p50 Ab (sc-7178; Santa Cruz Biotechnology).

RT-PCR

Total RNA from cells was reverse-transcribed with Superscript II reverse transcriptase (Invitrogen Life Technologies) and amplified by PCR. The following primers were used; FKN, a forward primer (5'-CACCTCGGC ATGACGAAAT) and a reverse primer (5'-TTGTCCACCCGCTTCTC AA-3'); MD-2, a forward primer (5'-ATGTTGCCATTTATTCTCTTTT CGACG) and a reverse primer (ATTGACATCACGGCGGTGAATGA TG-3'); TLR4, a forward primer (5'-AGCAGAGGAGAAAGCATCTATG ATC) and a reverse primer (GGTTTAGGCCCCAGAGTTTTTCTCC-3');

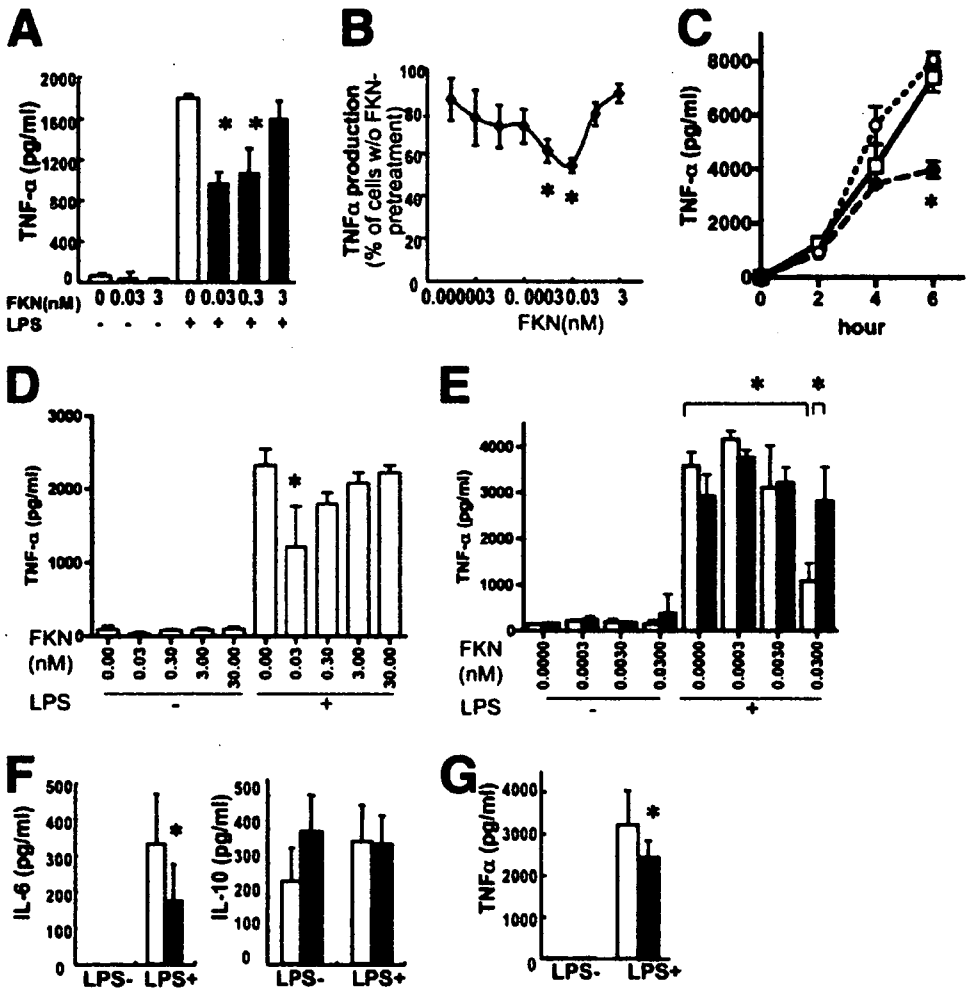

FIGURE 2. Pretreatment with recombinant FKN inhibited LPS-induced TNF-α production in macrophages. *A*, BMϕ were pretreated with FKN at indicated concentrations for 12 h and stimulated with LPS (100 ng/ml) for 6 h. Secretion of TNF-α in the culture medium was determined by ELISA and shown as an average plus 1 SD of four to eight independent cell preparations. *B*, RAW264.7 cells were pretreated with FKN at the indicated concentration for 12 h and stimulated with LPS (1 ng/ml) for 6 h. Secretion of TNF-α in the culture medium was determined by ELISA and shown as an average ± 1 SD of the percentage of cells without FKN pretreatment using three to eight independent cultures. *C*, RAW264.7 cells were pretreated with 0 nM (□), 0.03 nM (●), or 3 nM (○) FKN for 12 h and stimulated with LPS (1 ng/ml). Secretion of TNF-α in the culture medium was determined by ELISA at the indicated times after LPS stimulation and are shown as the average plus 1 SD. *D*, Culture plates were coated with indicated concentrations of FKN and RAW264.7 cells were cultured for 12 h and stimulated with LPS (1 ng/ml) for 6 h. Secretion of TNF-α was measured and shown as the average of eight cultures plus 1 SD. *E*, RAW264.7 cells were pretreated with FKN at the indicated concentrations in the presence of anti-CX3CR1 Ab (■ or control IgG (□) for 12 h and stimulated with LPS (1 ng/ml) for 6 h. Secretion of TNF-α was measured and shown as the average of three cultures plus 1 SD. *F*, BMϕ were pretreated with (■) or without (□) 0.03 nM FKN and then stimulated with 100 ng/ml LPS for 6 h. Secretions of IL-6 and IL-10 were measured and shown as an average plus 1 SD. *G*, BMϕ prepared from IL-10$^{-/-}$ mice (n = 10) were pretreated with (■) or without (□) 0.03 nM FKN and stimulated with 100 ng/ml LPS. Secretion of TNF-α was measured and shown as an average plus 1 SD. *, Statistically significant difference from cells without FKN- pretreatment; otherwise, compared data are indicated ($p < 0.05$).

CX3CR1, a forward primer (5′-CCGCCAACTCCATGAACAA) and a reverse primer (CGTCTGGATGATGCGGAAGTA-3′); PPAR-γ, a forward primer (5′-GATGCAAGGGTTTCTTCCGGAGAAC) and a reverse primer (TGGTGATTTGTCTGTTGTCTTTCC-3′); IL-23 p19, a forward primer (5′-GAACAAGATGCTGGATTGCAGAG) and a reverse primer (TGTGCGTTCCAGGCTAGCA-3′); and GAPDH, a forward primer (5′-AGCCAAACGGGTCATCATCTC) and a reverse primer (TGCCTGCT TCACCACCTTCTT-3′). For quantitative analysis, the SYBR Green PCR Kit (Applied Biosystems) was used according to the manufacturer's instructions in a model 7700 Sequence Detector (Applied Biosystems). The reaction mixture was amplified for GAPDH (95°C for 45 s, 60°C for 45 s, and 72°C for 45 s, in the order of denaturation, annealing, and extension, 40 cycles); MD-2 (90°C for 45 s, 58°C for 45 s, 72°C for 45 s, 40 cycles); TLR4 (94°C for 60 s, 60°C for 60 s, 72°C for 60 s, 40 cycles); CX3CR1 (94°C for 45 s, 58°C for 45 s, 72°C for 45 s, 40 cycles); FKN (94°C for 45 s, 58°C for 45 s, 72°C for 45 s, 40 cycles); PPAR-γ (95°C for 45 s, 55°C for 45 s, 72°C for 45 s, 40 cycles); and IL-23 p19 (95°C for 45 s, 60°C for 45 s, 72°C for 45 s, 40 cycles).

Preparation of nuclear extracts and EMSA

Cells were suspended in 200 μl of lysis buffer (10 mM HEPES (pH 7.9), 10 mM KCl, 0.1 mM EDTA, 0.1 mM EGTA, and 1 mM DTT) and kept on ice for 15 min followed by addition of 12.5 μl of 10% Nonidet P-40. After mixing and centrifugation (10,000 × g) for 3 min, the nuclear pellets obtained were resuspended in 25 μl of ice-cold nuclear extraction buffer (20 mM HEPES (pH 7.9), 400 mM NaCl, 1 mM EDTA, 1 mM EGTA, and 1 mM DTT) and kept on ice for 15 min with intermittent agitation. The samples were centrifuged and the supernatants were stored at −80°C until use. EMSAs were conducted using a Digoxigenin Gel Shift Kit (Roche Diagnostics) according to the manufacturer's instructions using 10 μg of the nuclear extracts. Quantification of bands was performed by densitometry using ATTO Densitograph version 4.0 software. For the supershift assay, we used an identical oligonucleotide probe labeled with [^{32}P]dCTP using a Klenow fragment. In brief, nuclear extracts (3 μg) were preincubated with 1 μg of anti-p50 or p65 Ab (sc-1190X, sc-372X; Santa Cruz Biotechnology) for 60 min at 4°C before addition of the labeled probe in

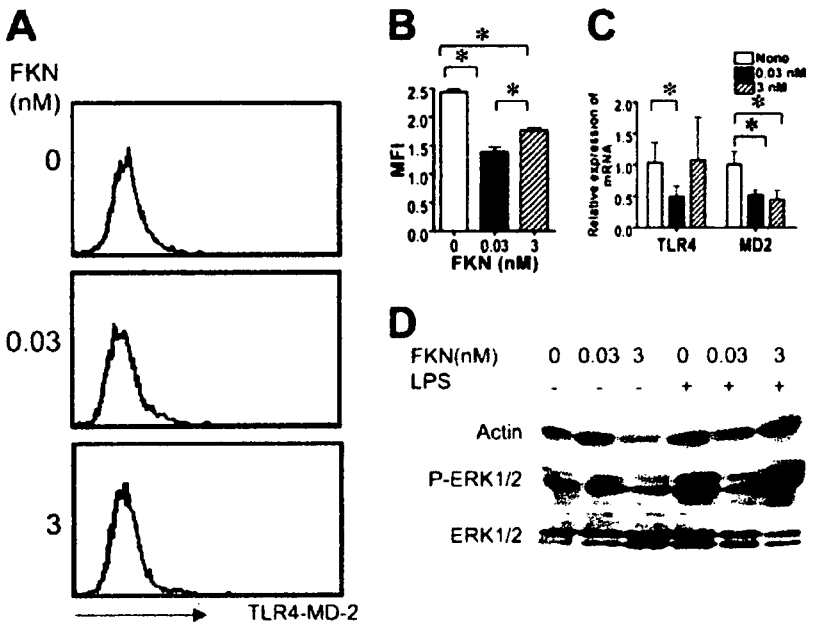

FIGURE 3. Pretreatment with FKN altered TLR4 and MD-2 expression and ERK1/2 phosphorylation. *A*, RAW264.7 cells were pretreated with the indicated concentrations of FKN for 12 h and stained with an Ab against the TLR4-MD-2 complex. Shaded histograms indicate staining with isotype control. *B*, The results in *A* are shown as the difference in mean fluorescence intensity from that of the isotype control. Results are shown as an average plus 1 SD of three experiments. *C*, RAW264.7 cells were pretreated with the indicated concentrations of FKN for 12 h and subjected to quantitative RT-PCR for TLR4 and MD-2. Results are shown as an average (n = 3 cultures) plus 1 SD of relative expression compared with the level of cells without FKN pretreatment. *, Statistically significant difference from cells without FKN pretreatment ($p < 0.05$). *D*, RAW264.7 cells were pretreated with the indicated concentration of FKN for 12 h and stimulated with LPS (1 ng/ml). Cell extracts were obtained after a 12-h pretreatment with FKN (LPS−) or after additional stimulation with LPS for 6 h (LPS+). Extracts were subjected to Western blotting to detect actin, phoshpo-ERK1/2, MAPK, and total ERK1/2. Representative data from four separate experiments are shown.

a total of 25 μl of binding buffer (10 mM HEPES (pH 7.8), 50 mM KCl, 1 mM EDTA, 5 mM MgCl2, 10% glycerol, and 1 μg of poly(dI:C)). After incubation, samples were fractionated on a 5% polyacrylamide gel in 25 mM Tris-Cl (pH 8.5), 190 mM glycine, and 1 mM EDTA. The gel was subsequently dried and visualized by autoradiography.

Quantification of NF-κB p65

The amount of NF-κB p65 in the nuclear protein fraction was measured using the TransFactor Extraction Kit and TransFactor Colorimetric Kit for NF-κB (BD Clontech). Amounts of NF-κB p65 were quantified as arbitrary units based on the colorimetric assay of serial dilutions of positive control samples.

Cell staining for detection of PPAR-γ and NF-κB p65

RAW264.7 cells were plated on Lab-Tek Chamber Slides (Nalge Nunc). After experimental treatment, cells were fixed by methanol, blocked with Block Ace (Dainippon Seiyaku) for 1 h, and incubated with rabbit anti-NF-κB p65 Ab (sc-372; Santa Cruz Biotechnology) and mouse anti-PPAR-γ mAb (sc-7273; Santa Cruz Biotechnology) or control normal mouse IgG (Cedarlane Laboratories) and normal rabbit IgG (Santa Cruz Biotechnology). Bound Ab were detected with goat anti-rabbit IgG tetramethylrhodamine isothiocyanate (Southern Biotechnology Associates) or biotinylated anti-mouse IgG (Vector Laboratories) and streptavidin-Alexa 488 (Invitrogen Life Technologies and Molecular Probes). Cells were then analyzed by confocal laser scanning microscopy (Zeiss LSM510; Zeiss).

Small interfering RNA (siRNA)

siRNA for mouse PPAR-γ and control siRNA were purchased from Santa Cruz Biotechnology. RAW264.7 cells were transfected with double-stranded siRNA at a final concentration of 100 nM using the MicroPorator MP-100 electroporation system (Digital BioTechnology) according to the manufacturer's instructions.

Immunostaining for 15d-PGJ2

RAW264.7 cells were stained with 2 μg/ml mouse anti-15d-PGJ2 mAb (11G2) or mouse control IgG overnight at 4°C as described previously (36) and then incubated with biotinylated anti-mouse IgG at a 1/400 dilution (Vector Laboratories) for 1 h followed by streptavidin-Alexa 488 at 1/1000 dilution for 1 h. After final washing and counterstaining with 4′,6-diamidino-2-phenylindole (DAPI), samples were evaluated using fluorescence microscopy (BX50/BXFLA; Olympus). Green (15d-PGJ2) and blue (nuclei) fluorescence images were captured separately from four fields of each culture randomly, and the stained area was measured using ImageJ software (distributed by the National Institutes of Health). Cellular expression of 15d-PGJ2 was determined as the green area (pixels) divided by blue area (pixels), which represents the number of cells in the image.

Statistics

The results were compared by the Mann-Whitney *U* test using the StatView II statistical program (Abacus Concepts) adapted for Mac OS.

Results

FKN and CX3CR1 are abundantly expressed in the intestine

Since CX3CR1-positive dendritic cells are abundantly distributed in the lamina propria of normal intestine (27), we initially examined the expression of the FKN ligand in the intestine. FKN was detected in epithelial as well as mesenchymal cells, especially in the proximal colon (Fig. 1*A*). FKN-positive mesenchymal cells, including myofibroblasts, were identified by double staining with anti-αsmooth musele actin as well as RT-PCR of murine myofibroblast cell lines which were established from the colon (our unpublished data). $CX3CR1^+F4/80^+$ macrophages were also found more frequently in the colon compared with the small intestine (Fig. 1*B*).

FKN attenuated LPS-induced secretion of TNF-α

To investigate the effect of FKN, we chose BMϕ and the mouse macrophage cell line RAW264.7 because both express the FKN receptor CX3CR1 (92 and 90%, respectively) and produce large amounts of TNF-α, an indicator of inflammation, in response to LPS stimulation for 6 h (Fig. 2). These cells were pretreated with FKN for 12 h and then stimulated with LPS. Although FKN itself did not induce secretion of TNF-α, pretreatment with FKN reduced the secretion of LPS-induced TNF-α in both BMϕ and RAW264.7 cells (Fig. 2, *A* and *B*). Of interest, ~0.003–0.03 nM FKN was optimal for this effect, and a higher concentration (3 nM) of FKN failed to attenuate TNF-α secretion (Fig. 2, *A* and *B*). Addition of an anti-FKN Ab during FKN pretreatment (0.03 nM) abolished its inhibitory effect, which indicated that the effect was due to FKN rather than any minor contaminant (data not shown). In the time course assay, less secretion of TNF-α in cells pretreated with 0.03 nM FKN became obvious 6 h after LPS challenge (Fig. 2*C*). Since FKN is expressed as a membrane-bound molecule as well as a soluble protein, we immobilized FKN on a plate and cultured RAW264.7 cells before LPS challenge. Immobilized FKN at a concentration of 0.03 nM also showed decreased TNF-α production by macrophages in response to LPS, whereas higher

concentrations did not show this effect (Fig. 2*D*). Washing the cells before LPS challenge reduced, at least in part, the inhibitory effect of FKN on TNF-α (data not shown), which indicated that both intracellular events and soluble factors released during pretreatment were involved in inhibition. To confirm that these dose-dependent, differential effects were mediated by a single FKN receptor, we added anti-CX3CR1 Ab when cells were pretreated with FKN. Reduction of TNF-α secretion in cells pretreated with 0.03 nM FKN was negated in the presence of anti-CX3CR1 Ab (Fig. 2*E*). This result indicated that the TNF-α suppressive effect was mediated by CX3CR1.

Pretreatment with 0.03 nM FKN also suppressed secretion of IL-6 from BMϕ induced by LPS, although the inhibitory effect was not as evident as that observed with levels of TNF-α in a 6-h culture (Fig. 2*F*). IL-12 production also was induced by LPS in BMϕ, but pretreatment with FKN did not affect its secretion significantly (data not shown). BMϕ constitutively produced IL-10 and pretreatment with FKN did not alter the levels of IL-10 in the culture supernatant, either without or with LPS (Fig. 2*F*). Similar effects of FKN pretreatment on cytokine production were seen in RAW264.7 cells. To examine the possible involvement of IL-10, BMϕ prepared from IL-10$^{-/-}$ mice were tested. Levels of TNF-α secretion after LPS stimulation in IL-10$^{-/-}$ BMϕ were >2-fold higher than in wild-type mice; however, pretreatment with FKN significantly decreased the level of TNF-α, although it did not reach 50% inhibition as seen in wild-type mice (Fig. 2*G*). Overall results showed that the LPS-induced TNF-α response was suppressed by pretreatment with 0.03 nM FKN and involvement of IL-10 in TNF-α suppression was only partial, if at all.

Pretreatment with FKN-modulated expression of TLR4

We next investigated whether FKN pretreatment might alter the expression of TLR4 and MD-2, molecules necessary for signal transduction from LPS. Although cell surface expression of the TLR4-MD-2 complex was not high in RAW264.7 cells, it significantly decreased in cells pretreated with 0.03 nM FKN as determined by flow cytometry (Fig. 3, *A* and *B*). Levels of TLR4 and MD-2 mRNA also decreased after pretreatment with 0.03 nM FKN (Fig. 3*C*). However, the mean fluorescence intensity of TLR4-MD-2 and mRNA levels of MD-2 in the cells treated with 3 nM FKN was still significantly lower than that of untreated control cells. Since TNF-α production by cells treated with 3 nM FKN was comparable to that of untreated cells, we assume that the surface expression level of TLR4-MD-2 was not the major factor that directly caused suppression of TNF-α secretion, although FKN does affect TLR4-MD-2 expression.

FKN attenuated ERK1/2 activation

Since MAPK phosphorylation occurs downstream of TLR4 signaling, the effect of FKN pretreatment was assessed. FKN itself induced ERK1/2 phosphorylation within 30 min; however, after 12 h (the time point of LPS addition), there was no significant activation of ERK1/2 in cells treated with either concentration of FKN (Fig. 3*D*). Phosphorylation of ERK1/2 was detected 30 min after stimulation with LPS irrespective of pretreatment with FKN (data not shown); however, 6 h after LPS challenge, MAPK phosphorylation was dramatically suppressed when cells were pretreated with 0.03 nM FKN. A higher concentration of FKN (3 nM) did not inhibit ERK phosphorylation (Fig. 3*D*), coinciding with the failure to suppress TNF-α secretion at this concentration. Phosphorylation of p38 was seen after stimulation with LPS; however, there is no difference between cells with or without FKN pretreatment (data not shown).

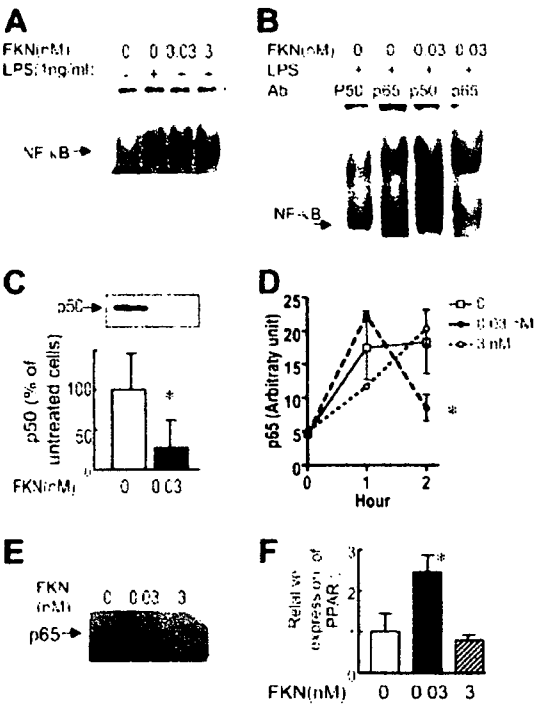

FIGURE 4. Pretreatment with FKN modulated activation of NF-κB. *A*, RAW264.7 cells were pretreated with the indicated concentration of FKN for 12 h and stimulated with LPS for 1 h. Nuclear extracts were subject to EMSA using a consensus NF-κB oligonucleotide probe. Specificity was confirmed by the loss of this band with the addition of unlabeled probe as a competitor. *B*, RAW264.7 cells were pretreated with or without 0.03 nM FKN and stimulated with 1 ng/ml LPS for 1 h. Nuclear extracts were subjected to supershifted EMSA in the presence of anti-NF-κB p65 or anti-p50 Ab. *C*, RAW264.7 cells were pretreated with 0.03 nM FKN and stimulated with 1 ng/ml LPS. Nuclear extracts were subject to Western blotting to detect p50 (*top panel*). The amount of p50 protein in three sets of experiments was quantified by densitometry and shown as the mean plus 1 SD normalized to the samples without pretreatment. *, Statistically significant difference from untreated cells ($p < 0.05$). *D*, RAW264.7 cells were pretreated with the indicated concentration of FKN for 12 h and stimulated with LPS for 1 or 2 h. Levels of p65 in the nuclear extract were measured. Results are shown as an average of eight independent cultures plus 1 SD. *, Statistically significant difference from untreated cells or cells treated with 3 nM FKN ($p < 0.05$). *E*, RAW264.7 cells were pretreated with the indicated concentration of FKN and stimulated with 1 ng/ml LPS for 2 h. Cytoplasmic extracts were immunoprecipitated with anti-PPAR-γ mAb and then subjected to blotting with anti-p65 Ab. *F*, RAW264.7 cells were pretreated with the indicated concentration of FKN for 12 h and mRNA extracts were subjected to RT-PCR for PPAR-γ. Results are shown as an average plus 1 SD of relative expression compared with the levels of nonpretreated cells from three independent preparations. *, Statistically significant difference from untreated cells or cells treated with 3 nM FKN ($p < 0.05$).

Effect of FKN pretreatment on NF-κB activation and induction of PPAR-γ

Inflammatory responses are closely linked to the activation of NF-κB, and LPS-induced transcription of TNF-α in macrophages is highly dependent on nuclear translocation of NF-κB. When RAW264.7 cells were stimulated with LPS, NF-κB activation was seen (Figs. 4*A* and 5*A*). Without LPS, very low levels of nuclear NF-κB were detected in RAW264.7 cells and treatment with either 0.03 nM or 3 nM FKN alone for 12 h did not show a significant effect on the status of NF-κB (data not shown). Unexpectedly, pretreatment with 0.03 nM FKN did not alter the amount of nuclear-translocated κB-binding protein for 1 h after LPS challenge

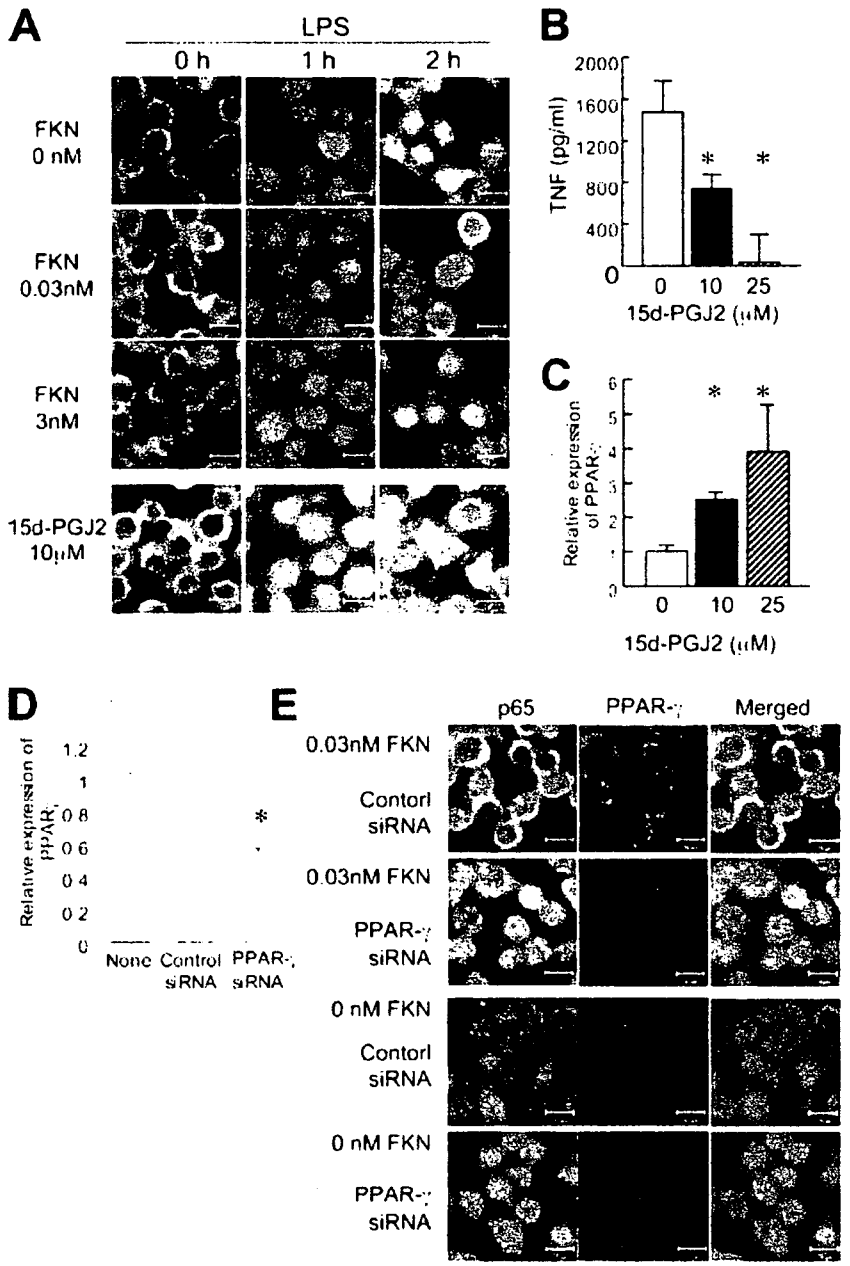

FIGURE 5. Pretreatment with FKN induced early export of NF-κB p65 from nuclei after stimulation with LPS in a PPAR-γ-dependent manner. *A*, RAW264.7 cells were pretreated with or without the indicated concentrations of either FKN or 15d-PGJ2 for 12 h and stimulated with 1 ng/ml LPS for either 1 or 2 h. Cells were then stained with anti-p65 (red) and anti-PPAR-γ (green) Ab; the merged images are shown. One representative result from four independent cultures in each condition is shown. *B*, RAW264.7 cells were pretreated with the indicated concentrations of 15d-PGJ2 for 12 h and stimulated with 1 ng/ml LPS for 6 h. Culture supernatants were subjected to TNF-α ELISA. Results are shown as the average plus 1 SD of four independent preparations. *C*, RAW264.7 cells were pretreated with the indicated concentrations of 15d-PGJ2 for 12 h and RNA extracts were subjected to quantitative RT-PCR for PPAR-γ. Results are shown as the mean plus 1 SD of the relative expression of the levels of nonpretreated cells of three independent preparations. *, Statistical significant differences from control cells without pretreatment. *D*, RAW264.7 cells were transfected with either PPAR-γ siRNA or control siRNA. Thirty-six hours after siRNA transfection, cells were treated with 0.03 nM FKN for 12 h. Total RNA was isolated and the levels of PPAR-γ mRNA were determined by quantitative RT-PCR. The fold induction was shown as the mRNA level relative to that of cells without siRNA transfection. Results are shown as the mean plus 1 SD of relative expression of the levels of nonpretreated cells from six independent preparations. *, Statistical significant differences from cells without transfection or transfected with control siRNA. *E*, RAW264.7 cells were transfected with either PPAR-γ or control siRNA. Thirty-six hours after transfection, cells were precultured with 0.03 nM FKN or without FKN (0 nM) for 12 h and then stimulated with 1 ng/ml LPS for 2 h. Cells were stained with anti-p65 (red) and anti-PPAR-γ (green) Ab. Representative results from four independent cultures in each condition are shown.

(Fig. 4*A*). Therefore, to find the mechanism of decreased TNF-α production, we performed supershift analysis focusing on the effect of pretreatment with 0.03 nM FKN. Without pretreatment, supershift was seen with both anti-p65 and anti-p50 Ab. In contrast, when cells were pretreated with 0.03 nM FKN, clear supershift was not seen with the anti-p50 Ab, while the NF-κB complex was supershifted with the anti-p65 Ab (Fig. 4*B*).

Decreased nuclear translocation of p50 protein in FKN-pretreated cells was confirmed by Western blotting (Fig. 4*C*). Furthermore, pretreatment with 0.03 nM FKN did not reduce but rather slightly increased the levels of p65 protein in the nucleus compared with those of untreated cells at the time point of 1 h after stimulation with LPS (Figs. 4*D* and 5*A*). Importantly, in these FKN-pretreated cells, p65 was rapidly eliminated from the nuclei 2 h after addition of LPS (Figs. 4*D* and 5*A*). In contrast, p65 remained in the nuclei at this time point in cells either without pretreatment or pretreated with 3 nM FKN (Figs. 4*D* and 5*A*).

From these results, we assumed that when cells were pretreated with 0.03 nM FKN, NF-κB p65 did not form a complex with p50 but with other molecules, which facilitated transport of p65 protein out of the nucleus. Since PPAR-γ was previously reported to have such a function (37), we performed immunoprecipitation analysis. We found that p65 protein and PPAR-γ were coprecipitated from cytoplasmic fractions 2 h after stimulation with LPS in cells that had been pretreated with 0.03 nM FKN (Fig. 4*E*). However, when cells were pretreated with 3 nM FKN, the p65-PPAR-γ complex was not detected (Fig. 4*E*). Immunofluorescence analysis also showed that nuclear p65 was efficiently moved to the cytoplasm with PPAR-γ in the cells pretreated with 0.03 nM FKN, while p65 remained in the nuclei in the cells without treatment or pretreated with 3 nM FKN 2 h after LPS stimulus (Fig. 5*A*). Since PPAR-γ is known to be a negative regulator of the inflammatory cytokine responses of macrophages (38, 39), we postulated that pretreatment with 0.03 nM FKN would induce and activate PPAR-γ and modulate NF-κB translocation, and finally attenuate the secretion of TNF-α. To examine this possibility, we determined the mRNA levels of PPAR-γ and found that the levels were enhanced after

a 12-h treatment with 0.03 nM FKN when compared with non-treated cells or those treated with 3 nM FKN (Fig. 4*F*).

Exogenous PPAR-γ ligand mimicked the effect of FKN

Since our results indicated the role of PPAR-γ activation in the anti-inflammatory effect of FKN, we pretreated cells with a natural PPAR-γ ligand and agonist, 15d-PGJ_2, instead of FKN. Pretreatment of RAW264.7 cells with 10 μM 15d-PGJ2 resulted in enhanced expression of PPAR-γ and nuclear translocation of p65 1 h after LPS stimulation, and then the p65 was rapidly cleared from nuclei at 2 h, as was observed in cells pretreated with 0.03 nM FKN (Fig. 5*A*). As a result, secretion of TNF-α decreased to 50% of untreated cells when cells were pretreated with 10 μM 15d-PGJ2 (Fig. 5*B*). The overall effect seen in the cells pretreated with 10 μM 15d-PGJ2 was similar to the effect of pretreatment with 0.03 nM FKN. Furthermore, we found that exogenous 15d-PGJ2 up-regulated PPAR-γ mRNA expression (Fig. 5*C*).

Effect of FKN on p65 redistribution depends on PPAR-γ

To confirm the key role of PPAR-γ in the effect of FKN on p65 redistribution, we used RNA interference. The introduction of siRNA for mouse PPAR-γ into RAW264.7 cells resulted in a 50% decrease in PPAR-γ mRNA levels compared with cells treated with control siRNA as determined by quantitative RT-PCR (Fig. 5*D*). As a result, PPAR-γ expression decreased (Fig. 5*E*) and the effect of pretreatment with 0.03 nM FKN was abolished; the NF-κB p65 subunit was retained in the nuclei 2 h after LPS challenge (Fig. 5*E*).

FKN enhances the levels of 15d-PGJ2

The exogenous PPAR-γ ligand 15d-PGJ2 up-regulated PPAR-γ mRNA expression and similarly altered NF-κB activation. Therefore, we investigated whether FKN itself could induce 15d-PGJ2. After a 2-h treatment with 0.03 nM FKN, 15d-PGJ2 was up-regulated and the enhanced expression was maintained for 12 h (Fig. 6, *A* and *B*). In contrast, expression levels of 15d-PGJ2 in cells treated with 3 nM of FKN were not significantly different from untreated control cells.

Induction of IL-23 by high concentrations of FKN

Since both 0.03 and 3 nM FKN showed a distinct effect in macrophages, we compared the mRNA levels of cytokines in cells pretreated with these low and high concentrations of FKN. Although there was no difference in expression of anti-inflammatory cytokines such as TGF-β or IL-10, we found that IL-23 p19 mRNA expression was significantly elevated in cells pretreated with 3 nM FKN and stimulated with LPS in comparison to those in cells not pretreated or pretreated with 0.03 nM FKN (Fig. 7*A*). Since induction of IL-23 p19 by high concentrations of FKN was blocked by anti-CX3CR1-neutralizing Ab, it was assumed to be mediated by CX3CR1 (Fig. 7*A*). Since 0.03 nM FKN as well as 3 nM FKN fully induced chemotaxis (data not shown), we assumed that signal transduction via CX3CR1 was sufficient at this relatively low concentration of FKN, and additional signals that promote IL-23 p19 expression might be induced at a higher concentration of FKN. This hypothesis was supported by the observation that addition of IL-23 after pretreatment with 0.03 nM FKN abolished the suppressive effect of 0.03 nM FKN (Fig. 7, *B* and *C*). Furthermore, early export of NF-κB p65 from the nuclei in the cells pretreated with 0.03 nM FKN was prevented in the presence of IL-23 (Fig. 7*C*). The significance of IL-23 in the action of 3 nM FKN was also supported by experiments using anti-IL-23 Ab. Both secretion of TNF-α and retention of NF-κB p65 in the nuclei after LPS stimulation in cells pretreated with 3 nM FKN were abolished in the presence of anti-IL-23 p19 Ab (Fig. 7, *D* and *E*).

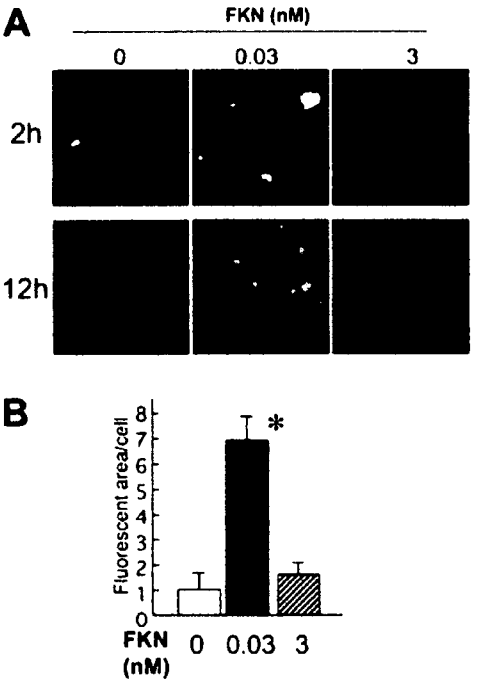

FIGURE 6. FKN increased the level of 15d-PGJ2. *A*, RAW264.7 cells were treated with the indicated concentration of FKN for 2 or 12 h and cells were stained with anti-15d-PGJ2 mAb (green). Nuclei were visualized by staining with DAPI (blue). *B*, RAW264.7 cells were treated with the indicated concentration of FKN for 12 h and stained with anti-15d-PGJ2 mAb and DAPI. The image as in *A* was captured and the levels of 15d-PGJ2 were measured as a ratio of green area to blue area. Results are shown as an average plus 1 SD of four measurements normalized to the value of cells without FKN treatment. Two other sets of experiments gave identical results. *, Statistically significant difference from cells without treatment 0 or treated with 3 nM FKN.

Discussion

This is the first report of an immunomodulatory effect of FKN independent of its well-investigated function as a chemokine and adhesion molecule. The mechanism of the anti-inflammatory effect of relatively low concentrations of FKN involved activation of PPAR-γ by induction of its ligand, 15d-PGJ2, and alteration of signaling via ERK1/2 and NF-κB. These novel immune regulation systems in macrophages are discussed below.

Up-regulation of FKN expression in inflammatory tissue has drawn attention to its potential as a target of anti-inflammatory treatment for various autoimmune diseases. However, FKN is constitutively produced by intestinal epithelial cells and its receptor, CX3CR1, is expressed on tissue-resident dendritic cells and macrophages in the intestine and CNS. In the case of murine intestine, we found that a considerable amount of FKN was expressed in the colon, and colonic myofibroblasts were also another significant source of FKN (our unpublished data). Of note, the resident macrophages of the intestine are hyporesponsive to inflammatory stimuli with bacterial components such as LPS. It is evident, especially in the large intestine, that macrophage-like cells in the colonic lamina propria are mostly anergic in response to endotoxin, in contrast to the vigorous cytokine production by circulating monocyte via the same stimuli (33). For heavy colonization of indigenous Gram-negative bacteria in the colon, hyporesponsiveness of macrophages would be important for maintaining homeostasis of

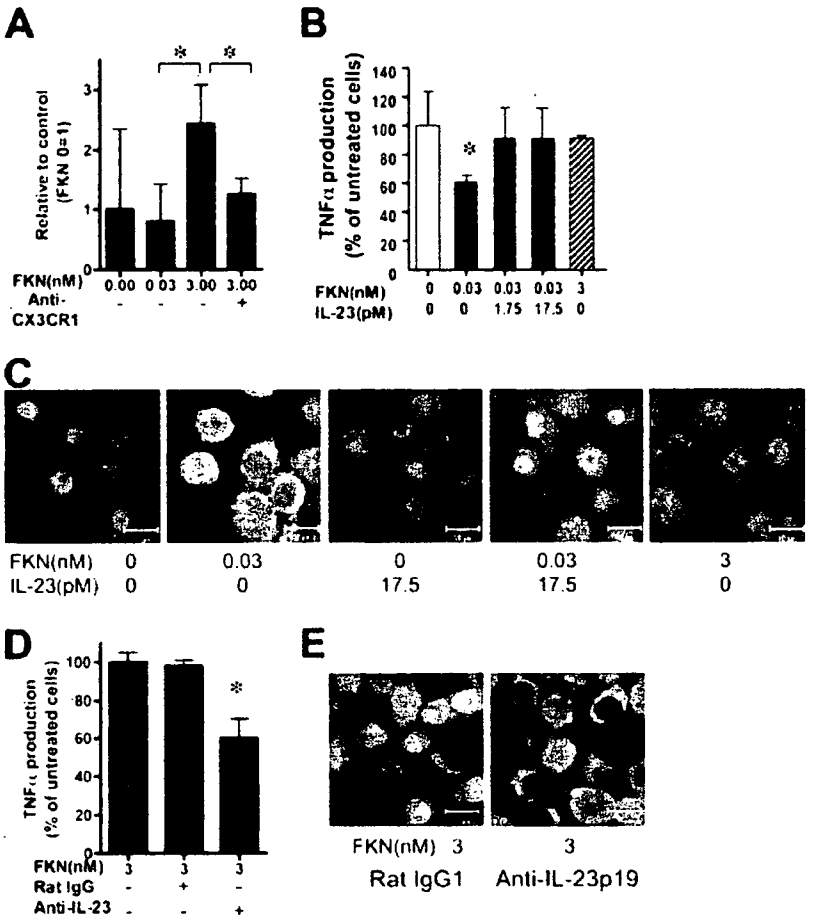

FIGURE 7. Pretreatment with a high concentration of FKN up-regulated mRNA for IL-23 p19 after LPS stimulation and facilitated TNF-α secretion. *A*, RAW264.7 cells were treated with the indicated concentration of FKN for 12 h with or without anti-CX3CR1 Ab or control IgG and stimulated with LPS (1 ng/ml) for 6 h. Cells then were subjected to quantitative RT-PCR for IL-23 p19. *, Indicates that the difference from cells treated with 0.03 nM FKN is statistically significant ($p < 0.05$). *B*, RAW264.7 cells were pretreated with the indicated amount of FKN and then stimulated with LPS in the presence of various amounts of IL-23 for 6 h. Secretion of TNF-α in culture supernatants was measured by ELISA. Results are shown as an average plus 1 SD of the percentage of the value of cells without FKN pretreatment from six independent cultures. *, Statistically significant difference from other experimental conditions shown ($p < 0.05$). *C*, RAW264.7 cells were pretreated with or without 0.03 or 3 nM FKN for 12 h and then stimulated with LPS (0.03 nM) in the absence or presence of IL-23 (17.5 pM) for 2 h. Cells then were stained with anti-p65 (red) and anti-PPAR-γ (green) Ab; the merged images are shown. *D*, RAW264.7 cells were pretreated with 3 nM FKN for 12 h and then stimulated with LPS (1 ng/ml) with or without anti-IL-23 Ab or control IgG for 6 h. Results are shown as the average plus 1 SD of the percentage of cells without FKN pretreatment from six independent cultures. *, Statistically significant difference from other experimental conditions shown ($p < 0.05$). *E*, RAW264.7 cells were pretreated with 3 nM FKN for 12 h and then stimulated with LPS (1 ng/ml) with or without anti-IL-23 Ab for2 h. Cells were then stained with anti-p65 Ab.

mucosal immunity. The possibility that FKN participates in rendering macrophages hyporesponsive to LPS was first demonstrated in this study. This effect of FKN is reminiscent of the phenomenon of endotoxin tolerance, i.e., exposure of macrophages to LPS induces a hyporesponsive state to a second challenge with LPS. Although various mechanisms are involved in endotoxin tolerance, few studies have reported the mechanism of hyporesponsiveness of intestinal macrophages at the molecular level. For example, the IκBNS is a key molecule that inhibits IL-12 and IL-6 production in murine intestinal macrophages, although this mechanism was irrelevant to TNF-α secretion (31). Lack of MD-2 expression in intestinal myeloid-type cells (33) or epithelial cells (40) also has been postulated as a mechanism for the limited responses to LPS derived from indigenous flora. However, in our study, FKN did not down-regulate expression of the TLR4-MD-2 completely, although the level of mRNA was significantly reduced. Furthermore, IL-10 was not entirely responsible for the suppression of TNF-α. We also found that Bcl3 and TNFR-associated factor 6 were not significantly involved in this system (our unpublished data). Thus, the mechanism of inhibition of LPS-triggered TNF-α secretion by FKN was distinct from those mechanisms already known for the phenomenon of endotoxin tolerance.

In the current study, we found that FKN up-regulated PPAR-γ expression with its ligand and reduced production of TNF-α. This was also associated with modulation of subunit usage of NF-κB; the p65 subunit did not form a complex with the p50 subunit as seen in the LPS-challenged cells without FKN pretreatment. Instead, PPAR-γ formed a complex with the p65 subunit, which seemed to facilitate early export of p65 from nuclei. Inhibition of NF-κB activation by cytoplasmic protein IκB, which prevents nuclear translocation of p65, is not likely to be a major factor in the FKN system because nuclear translocation of p65 took place 1 h after LPS stimulation in our experiment. Our results indicated that the p65 subunit was once translocated into the nucleus, but in complex with PPAR-γ was rapidly exported. We are not the first to describe the function of PPAR-γ in regulating inflammatory responses. When intestinal epithelial cells were treated with a strain of commensal bacteria, *Bacteroides thetaiotaomicron*, PPAR-γ underwent nucleocytoplasmic redistribution in complex with p65, which ultimately caused the attenuation of IL-8 expression induced by pathogenic *Salmonella enteritidis* (37). The role of PPAR-γ as an anti-inflammatory factor is well known; activation of PPAR-γ inhibited the expression of various cytokines in monocytes and macrophages, principally by preventing the activation of NF-κB; however, its mechanism of action is not clear (38, 39, 41). An endogenous ligand of PPAR-γ, 15d-PGJ2, a metabolite from PGD_2 (36), exerts a strong anti-inflammatory effect on macrophages. In our experiment, the effect of exogenous 15d-PGJ2 on NF-κB activation and cytokine production was very similar to that of FKN, especially at 10 μM. Since induction of 15d-PGJ2 was observed after FKN treatment, it is likely that up-regulation of 15d-PGJ2 elicited the anti-inflammatory effect in our experimental system. It was initially reported that 15d-PGJ2 affected NF-κB activation in a PPAR-γ-dependent manner (39); however, a PPAR-γ-independent pathway was also reported later (42–45). Based on the results that cellular 15d-PGJ2 was up-regulated rapidly after pretreatment with FKN and remained up-regulated for 12 h and that expression of PPAR-γ mRNA was enhanced by exogenous 15d-PGJ2 in macrophages, FKN most probably increased the level of 15d-PGJ2 first, followed by up-regulation of PPAR-γ, which

resulted in the modulation of NF-κB activation. Indeed, our experiment using PPAR-γ siRNA clearly showed that the anti-inflammatory effect of FKN depends on the presence of PPAR-γ, although we think it is still possible that FKN-induced 15d-PGJ2 or other unknown anti-inflammatory signaling pathways, independent of PPAR-γ, may directly affect expression of TLR4-MD-2 and phosphorylation of ERK1/2.

It is notable that the anti-inflammatory effect of FKN was seen when cells were pretreated with FKN at a concentration of 0.03 nM but not at 3 nM. We clearly observed a dose-dependent difference in every assay of signaling systems, such as ERK1/2 phosphorylation, complex formation of NF-κB p65 and PPAR-γ, early export of p65 from nuclei, induction of PPAR-γ mRNA, as well as up-regulation of 15d-PGJ2; all supported inhibition of TNF-α secretion by 0.03 nM but not 3 nM FKN. We could only partially clarify the mechanisms of the anti-inflammatory effect specific to this concentration of FKN. Since chemotaxis was fully triggered at 0.03 nM FKN, this concentration of FKN was sufficient to transduce classical signaling via CX3CR1. It also indicated the probability that 3 nM FKN induced additional signaling pathways, and our result demonstrated that IL-23 counteracts the anti-inflammatory effect of FKN. We assumed that this duality might be caused by differential rates of occupancy and dimerization of CX3CR1. It is possible that the proinflammatory action of FKN may depend partially on the induction of IL-23, which would be up-regulated in the cells exposed to a higher than physiological concentration of FKN. It has been shown that IL-23 is a potent activator of macrophages that enhances TNF-α expression (46) and transgenic expression of IL-23 p19 induces multiorgan inflammation (47); however, its regulatory role in mucosal inflammation is either proinflammatory (48) or anti-inflammatory (49) according to the disease models used. Such dose-dependent dual effects of FKN were not described in microglia, in which FKN was capable of attenuating LPS-induced TNF-α secretion in a dose-dependent manner (17). Differences in surface expression of LPS receptors, such as low CD14 in microglia (50), might cause this cell-specific effect. A detailed mechanism of interaction between IL-23 and FKN in macrophages is now under investigation in our laboratory. The reason why FKN has these specific effects at certain concentrations may lie in the unrevealed general mechanism of chemotaxis. Chemotaxis occurs when cells recognize a "concentration gradient" and move toward the area of higher concentration; however, the sensor mechanism for the concentration gradient is largely unknown. To determine the direction of chemotaxis, a single cell may have sensors for both low and high concentrations of ligands that mediate different signals in a three-dimensional intracellular mapping system. Our finding of dose-dependent, differential effects through CX3CR1 might represent the nature of chemokine receptors. With respect to physiological relevance, it is reasonable that cells respond in a distinct manner in the milieu of low and high concentrations of chemokine. For example, macrophages in the intestine at steady state exposed to a relatively low physiological level of FKN acquired hyporesponsiveness to LPS, which prevented an excessive inflammatory response to commensal flora. When inflammation occurs and higher concentrations of FKN and additional inflammatory cytokines are produced, newly recruited inflammatory macrophages have the potential to fully respond to produce TNF-α as an immune defense mechanism. According to previous reports, concentrations of FKN in the plasma of healthy humans were <0.03 nM (1 ng/ml) and approached 1 nM (30 ng/ml) in the plasma of patients with inflammatory airway disease (51). Thus, this study used both low and high concentrations of FKN, which may approximate those of steady-state and inflammatory situations, respectively.

Our results showed the anti-inflammatory effect of FKN, which is constitutively expressed in the colon where a high level of PPAR-γ is also expressed (52). The presence of soluble factors is known to suppress the inflammatory reaction of macrophages (32). We propose that the physiological concentration of FKN may be one such factor that maintains immune homeostasis in the intestine.

Acknowledgments

We thank Drs. Sachiko Akashi and Kensuke Miyake at Tokyo University for providing us with mAb SA15-21.

Disclosures

The authors have no financial conflict of interest.

References

1. Bazan, J. F., K. B. Bacon, G. Hardiman, W. Wang, K. Soo, D. Rossi, D. R. Greaves, A. Zlotnik, and T. J. Schall. 1997. A new class of membrane-bound chemokine with a CX3C motif. *Nature* 385: 640–644.
2. Garton, K. J., P. J. Gough, C. P. Blobel, G. Murphy, D. R. Greaves, P. J. Dempsey, and E. W. Raines. 2001. Tumor necrosis factor-α-converting enzyme (ADAM17) mediates the cleavage and shedding of fractalkine (CX3CL1). *J. Biol. Chem.* 276: 37993–38001.
3. Tsou, C. L., C. A. Haskell, and I. F. Charo. 2001. Tumor necrosis factor-α-converting enzyme mediates the inducible cleavage of fractalkine. *J. Biol. Chem.* 276: 44622–44626.
4. Fraticelli, P., M. Sironi, G. Bianchi, D. D'Ambrosio, C. Albanesi, A. Stoppacciaro, M. Chieppa, P. Allavena, L. Ruco, G. Girolomoni, et al. 2001. Fractalkine (CX3CL1) as an amplification circuit of polarized Th1 responses. *J. Clin. Invest.* 107: 1173–1181.
5. Imaizumi, T., H. Yoshida, and K. Satoh. 2004. Regulation of CX3CL1/fractalkine expression in endothelial cells. *J. Atheroscler. Thromb.* 11: 15–21.
6. Fujimoto, K., T. Imaizumi, H. Yoshida, S. Takanashi, K. Okumura, and K. Satoh. 2001. Interferon-γ stimulates fractalkine expression in human bronchial epithelial cells and regulates mononuclear cell adherence. *Am. J. Respir. Cell Mol. Biol.* 25: 233–238.
7. Umehara, H., E. T. Bloom, T. Okazaki, Y. Nagano, O. Yoshie, and T. Imai. 2004. Fractalkine in vascular biology: from basic research to clinical disease. *Arterioscler. Thromb. Vasc. Biol.* 24: 34–40.
8. Fong, A. M., L. A. Robinson, D. A. Steeber, T. F. Tedder, O. Yoshie, T. Imai, and D. D. Patel. 1998. Fractalkine and CX3CR1 mediate a novel mechanism of leukocyte capture, firm adhesion, and activation under physiologic flow. *J. Exp. Med.* 188: 1413–1419.
9. Imai, T., K. Hieshima, C. Haskell, M. Baba, M. Nagira, M. Nishimura, M. Kakizaki, S. Takagi, H. Nomiyama, T. J. Schall, and O. Yoshie. 1997. Identification and molecular characterization of fractalkine receptor CX3CR1, which mediates both leukocyte migration and adhesion. *Cell* 91: 521–530.
10. Combadiere, C., J. Gao, H. L. Tiffany, and P. M. Murphy. 1998. Gene cloning, RNA distribution, and functional expression of mCX3CR1, a mouse chemotactic receptor for the CX3C chemokine fractalkine. *Biochem. Biophys. Res. Commun.* 253: 728–732.
11. Ancuta, P., R. Rao, A. Moses, A. Mehle, S. K. Shaw, F. W. Luscinskas, and D. Gabuzda. 2003. Fractalkine preferentially mediates arrest and migration of $CD16^+$ monocytes. *J. Exp. Med.* 197: 1701–1707.
12. Nanki, T., T. Imai, K. Nagasaka, Y. Urasaki, Y. Nonomura, K. Taniguchi, K. Hayashida, J. Hasegawa, O. Yoshie, and N. Miyasaka. 2002. Migration of CX3CR1-positive T cells producing type 1 cytokines and cytotoxic molecules into the synovium of patients with rheumatoid arthritis. *Arthritis Rheum.* 46: 2878–2883.
13. Nishimura, M., H. Umehara, T. Nakayama, O. Yoneda, K. Hieshima, M. Kakizaki, N. Dohmae, O. Yoshie, and T. Imai. 2002. Dual functions of fractalkine/CX3C ligand 1 in trafficking of $perforin^+$/granzyme B^+ cytotoxic effector lymphocytes that are defined by CX3CR1 expression. *J. Immunol.* 168: 6173–6180.
14. Papadopoulos, E. J., D. J. Fitzhugh, C. Tkaczyk, A. M. Gilfillan, C. Sassetti, D. D. Metcalfe, and S. T. Hwang. 2000. Mast cells migrate, but do not degranulate, in response to fractalkine, a membrane-bound chemokine expressed constitutively in diverse cells of the skin. *Eur. J. Immunol.* 30: 2355–2361.
15. Hatori, K., A. Nagai, R. Heisel, J. K. Ryu, and S. U. Kim. 2002. Fractalkine and fractalkine receptors in human neurons and glial cells. *J. Neurosci. Res.* 69: 418–426.
16. Maciejewski-Lenoir, D., S. Chen, L. Feng, R. Maki, and K. B. Bacon. 1999. Characterization of fractalkine in rat brain cells: migratory and activation signals for CX3CR-1-expressing microglia. *J. Immunol.* 163: 1628–1635.
17. Mizuno, T., J. Kawanokuchi, K. Numata, and A. Suzumura. 2003. Production and neuroprotective functions of fractalkine in the central nervous system. *Brain Res.* 979: 65–70.
18. Volin, M. V., J. M. Woods, M. A. Amin, M. A. Connors, L. A. Harlow, and A. E. Koch. 2001. Fractalkine: a novel angiogenic chemokine in rheumatoid arthritis. *Am. J. Pathol.* 159: 1521–1530.
19. Muehlhoefer, A., L. J. Saubermann, X. Gu, K. Luedtke-Heckenkamp, R. Xavier, R. S. Blumberg, D. K. Podolsky, R. P. MacDermott, and H. C. Reinecker. 2000.

Fractalkine is an epithelial and endothelial cell-derived chemoattractant for intraepithelial lymphocytes in the small intestinal mucosa. *J. Immunol.* 164: 3368–3376.
20. Combadiere, C., S. Potteaux, J. L. Gao, B. Esposito, S. Casanova, E. J. Lee, P. Debre, A. Tedgui, P. M. Murphy, and Z. Mallat. 2003. Decreased atherosclerotic lesion formation in CX3CR1/apolipoprotein E double knockout mice. *Circulation* 107: 1009–1016.
21. Raychaudhuri, S. P., W. Y. Jiang, and E. M. Farber. 2001. Cellular localization of fractalkine at sites of inflammation: antigen-presenting cells in psoriasis express high levels of fractalkine. *Br. J. Dermatol.* 144: 1105–1113.
22. Suzuki, F., T. Nanki, T. Imai, H. Kikuchi, S. Hirohata, H. Kohsaka, and N. Miyasaka. 2005. Inhibition of CX3CL1 (fractalkine) improves experimental autoimmune myositis in SJL/J mice. *J. Immunol.* 175: 6987–6996.
23. Cockwell, P., S. J. Chakravorty, J. Girdlestone, and C. O. Savage. 2002. Fractalkine expression in human renal inflammation. *J. Pathol.* 196: 85–90.
24. Boehme, S. A., F. M. Lio, D. Maciejewski-Lenoir, K. B. Bacon, and P. J. Conlon. 2000. The chemokine fractalkine inhibits Fas-mediated cell death of brain microglia. *J. Immunol.* 165: 397–403.
25. Cook, D. N., S. C. Chen, L. M. Sullivan, D. J. Manfra, M. T. Wiekowski, D. M. Prosser, G. Vassileva, and S. A. Lira. 2001. Generation and analysis of mice lacking the chemokine fractalkine. *Mol. Cell. Biol.* 21: 3159–3165.
26. Geissmann, F., S. Jung, and D. R. Littman. 2003. Blood monocytes consist of two principal subsets with distinct migratory properties. *Immunity* 19: 71–82.
27. Niess, J. H., S. Brand, X. Gu, L. Landsman, S. Jung, B. A. McCormick, J. M. Vyas, M. Boes, H. L. Ploegh, J. G. Fox, D. R. Littman, and H. C. Reinecker. 2005. CX3CR1-mediated dendritic cell access to the intestinal lumen and bacterial clearance. *Science* 307: 254–258.
28. Fogg, D. K., C. Sibon, C. Miled, S. Jung, P. Aucouturier, D. R. Littman, A. Cumano, and F. Geissmann. 2006. A clonogenic bone marrow progenitor specific for macrophages and dendritic cells. *Science* 311: 83–87.
29. Yrlid, U., C. D. Jenkins, and G. G. MacPherson. 2006. Relationships between distinct blood monocyte subsets and migrating intestinal lymph dendritic cells in vivo under steady-state conditions. *J. Immunol.* 176: 4155–4162.
30. Lucas, A. D., N. Chadwick, B. F. Warren, D. P. Jewell, S. Gordon, F. Powrie, and D. R. Greaves. 2001. The transmembrane form of the CX3CL1 chemokine fractalkine is expressed predominantly by epithelial cells in vivo. *Am. J. Pathol.* 158: 855–866.
31. Hirotani, T., P. Y. Lee, H. Kuwata, M. Yamamoto, M. Matsumoto, I. Kawase, S. Akira, and K. Takeda. 2005. The nuclear IκB protein IκBNS selectively inhibits lipopolysaccharide-induced IL-6 production in macrophages of the colonic lamina propria. *J. Immunol.* 174: 3650–3657.
32. Smythies, L. E., M. Sellers, R. H. Clements, M. Mosteller-Barnum, G. Meng, W. H. Benjamin, J. M. Orenstein, and P. D. Smith. 2005. Human intestinal macrophages display profound inflammatory anergy despite avid phagocytic and bacteriocidal activity. *J. Clin. Invest.* 115: 66–75.
33. Shirai, Y., M. Hashimoto, R. Kato, Y. I. Kawamura, T. Kirikae, H. Yano, J. Takashima, Y. Kirihara, Y. Saito, M. A. Fujino, and T. Dohi. 2004. Lipopolysaccharide induces CD25-positive, IL-10-producing lymphocytes without secretion of proinflammatory cytokines in the human colon: low MD-2 mRNA expression in colonic macrophages. *J. Clin. Immunol.* 24: 42–52.
34. Zujovic, V., J. Benavides, X. Vige, C. Carter, and V. Taupin. 2000. Fractalkine modulates TNF-α secretion and neurotoxicity induced by microglial activation. *Glia* 29: 305–315.
35. Zujovic, V., N. Schussler, D. Jourdain, D. Duverger, and V. Taupin. 2001. In vivo neutralization of endogenous brain fractalkine increases hippocampal TNFα and 8-isoprostane production induced by intracerebroventricular injection of LPS. *J. Neuroimmunol.* 115: 135–143.
36. Shibata, T., M. Kondo, T. Osawa, N. Shibata, M. Kobayashi, and K. Uchida. 2002. 15-deoxy-Δ 12,14-prostaglandin J2: a prostaglandin D_2 metabolite generated during inflammatory processes. *J. Biol. Chem.* 277: 10459–10466.
37. Kelly, D., J. I. Campbell, T. P. King, G. Grant, E. A. Jansson, A. G. Coutts, S. Pettersson, and S. Conway. 2004. Commensal anaerobic gut bacteria attenuate inflammation by regulating nuclear-cytoplasmic shuttling of PPAR-γ and RelA. *Nat. Immunol.* 5: 104–112.
38. Jiang, C., A. T. Ting, and B. Seed. 1998. PPAR-γ agonists inhibit production of monocyte inflammatory cytokines. *Nature* 391: 82–86.
39. Ricote, M., A. C. Li, T. M. Willson, C. J. Kelly, and C. K. Glass. 1998. The peroxisome proliferator-activated receptor-γ is a negative regulator of macrophage activation. *Nature* 391: 79–82.
40. Abreu, M. T., P. Vora, E. Faure, L. S. Thomas, E. T. Arnold, and M. Arditi. 2001. Decreased expression of toll-like receptor-4 and MD-2 correlates with intestinal epithelial cell protection against dysregulated proinflammatory gene expression in response to bacterial lipopolysaccharide. *J. Immunol.* 167: 1609–1616.
41. Glass, C. K., and S. Ogawa. 2006. Combinatorial roles of nuclear receptors in inflammation and immunity. *Nat. Rev. Immunol.* 6: 44–55.
42. Straus, D. S., G. Pascual, M. Li, J. S. Welch, M. Ricote, C. H. Hsiang, L. L. Sengchanthalangsy, G. Ghosh, and C. K. Glass. 2000. 15-deoxy-Δ12,14-prostaglandin J2 inhibits multiple steps in the NF-κB signaling pathway. *Proc. Natl. Acad. Sci. USA* 97: 4844–4849.
43. Rossi, A., P. Kapahi, G. Natoli, T. Takahashi, Y. Chen, M. Karin, and M. G. Santoro. 2000. Anti-inflammatory cyclopentenone prostaglandins are direct inhibitors of IκB kinase. *Nature* 403: 103–108.
44. Thieringer, R., J. E. Fenyk-Melody, C. B. Le Grand, B. A. Shelton, P. A. Detmers, E. P. Somers, L. Carbin, D. E. Moller, S. D. Wright, and J. Berger. 2000. Activation of peroxisome proliferator-activated receptor γ does not inhibit IL-6 or TNF-α responses of macrophages to lipopolysaccharide in vitro or in vivo. *J. Immunol.* 164: 1046–1054.
45. Giri, S., R. Rattan, A. K. Singh, and I. Singh. 2004. The 15-deoxy-Δ12,14-prostaglandin J2 inhibits the inflammatory response in primary rat astrocytes via down-regulating multiple steps in phosphatidylinositol 3-kinase-Akt-NF-κB-p300 pathway independent of peroxisome proliferator-activated receptor γ. *J. Immunol.* 173: 5196–5208.
46. Cua, D. J., J. Sherlock, Y. Chen, C. A. Murphy, B. Joyce, B. Seymour, L. Lucian, W. To, S. Kwan, T. Churakova, et al. 2003. Interleukin-23 rather than interleukin-12 is the critical cytokine for autoimmune inflammation of the brain. *Nature* 421: 744–748.
47. Wiekowski, M. T., M. W. Leach, E. W. Evans, L. Sullivan, S. C. Chen, G. Vassileva, J. F. Bazan, D. M. Gorman, R. A. Kastelein, S. Narula, and S. A. Lira. 2001. Ubiquitous transgenic expression of the IL-23 subunit p19 induces multiorgan inflammation, runting, infertility, and premature death. *J. Immunol.* 166: 7563–7570.
48. Uhlig, H. H., B. S. McKenzie, S. Hue, C. Thompson, B. Joyce-Shaikh, R. Stepankova, N. Robinson, S. Buonocore, H. Tlaskalova-Hogenova, D. J. Cua, and F. Powrie. 2006. Differential activity of IL-12 and IL-23 in mucosal and systemic innate immune pathology. *Immunity* 25: 309–318.
49. Becker, C., H. Dornhoff, C. Neufert, M. C. Fantini, S. Wirtz, S. Huebner, A. Nikolaev, H. A. Lehr, A. J. Murphy, D. M. Valenzuela, et al. 2006. Cutting edge: IL-23 cross-regulates IL-12 production in T cell-dependent experimental colitis. *J. Immunol.* 177: 2760–2764.
50. Guillemin, G. J., and B. J. Brew. 2004. Microglia, macrophages, perivascular macrophages, and pericytes: a review of function and identification. *J. Leukocyte Biol.* 75: 388–397.
51. Ruth, J. H., M. V. Volin, G. K. Haines, III, D. C. Woodruff, K. J. Katschke, Jr., J. M. Woods, C. C. Park, J. C. Morel, and A. E. Koch. 2001. Fractalkine, a novel chemokine in rheumatoid arthritis and in rat adjuvant-induced arthritis. *Arthritis Rheum.* 44: 1568–1581.
52. Mansen, A., H. Guardiola-Diaz, J. Rafter, C. Branting, and J. A. Gustafsson. 1996. Expression of the peroxisome proliferator-activated receptor (PPAR) in the mouse colonic mucosa. *Biochem. Biophys. Res. Commun.* 222: 844–851.

Research article

Association of the diplotype configuration at the *N*-acetyltransferase 2 gene with adverse events with co-trimoxazole in Japanese patients with systemic lupus erythematosus

Makoto Soejima[1], Tomoko Sugiura[1], Yasushi Kawaguchi[1], Manabu Kawamoto[1], Yasuhiro Katsumata[1], Kae Takagi[1], Ayako Nakajima[1], Tadayuki Mitamura[2], Akio Mimori[3], Masako Hara[1] and Naoyuki Kamatani[1]

[1]Institute of Rheumatology, Tokyo Women's Medical University School of Medicine, Kawada-cho, Shinjuku-ku, Tokyo 162-0054, Japan
[2]Department of Hematology and Rheumatology, JR Tokyo General Hospital, Yoyogi, Shibuya-ku, Tokyo, 151-8528, Japan
[3]Department of Rheumatology, International Medical Center of Japan, Toyama, Shinjuku-ku, Tokyo, 162-8855, Japan

Corresponding author: Yasushi Kawaguchi, y-kawa@ior.twmu.ac.jp

Received: 17 Dec 2006 Revisions requested: 16 Jan 2007 Revisions received: 11 Feb 2007 Accepted: 3 Mar 2007 Published: 3 Mar 2007

Arthritis Research & Therapy 2007, **9**:R23 (doi:10.1186/ar2134)
This article is online at: http://arthritis-research.com/content/9/2/R23

Abstract

Although co-trimoxazole (trimethoprim-sulphamethoxazole) is an effective drug for prophylaxis against and treatment of *Pneumocystis* pneumonia, patients often experience adverse events with this combination, even at prophylactic doses. With the aim being to achieve individual optimization of co-trimoxazole therapy in patients with systemic lupus erythematosus (SLE), we investigated genetic polymorphisms in the *NAT2* gene (which encodes the metabolizing enzyme of sulphamethoxazole). Of 166 patients with SLE, 54 patients who were hospitalized and who received prophylactic doses of co-trimoxazole were included in the cohort study. Adverse events occurred in 18 patients; only two experienced severe adverse events that lead to discontinuation of the drug. These two patients and three additional ones with severe adverse events (from other institutions) were added to form a cohort sample and were analyzed in a case-control study. Genotype was determined using TaqMan methods, and haplotype was inferred using the maximum-likelihood method. In the cohort study, adverse events occurred more frequently in those without the *NAT2*4* haplotype (5/7 [71.4%]) than in those with at least one *NAT2*4* haplotype (13/47 [27.7%]; $P = 0.034$; relative risk = 2.58, 95% confidence interval = 1.34–4.99). In the case-control study the proportion of patients without *NAT2*4* was significantly higher among those with severe adverse events (3/5 [60%]) than those without severe adverse events (6/52 [11.5%]; $P = 0.024$; odds ratio = 11.5, 95% confidence interval = 1.59–73.39). We conclude that lack of *NAT2*4* haplotype is associated with adverse events with co-trimoxazole in Japanese patients with SLE.

Introduction

Co-trimoxazole (trimethoprim-sulphamethoxazole) is an effective drug in the prevention and treatment of *Pneumocystis* pneumonia [1,2], a life-threatening condition that mainly occurs in immunodeficient patients. Usage of the drug was recently extended to patients with connective tissue disease, including systemic lupus erythematosus (SLE) [3]. Although co-trimoxazole was confirmed to have prophylactic effect against *Pneumocystis* pneumonia in SLE patients, it often causes adverse events, even at prophylactic doses. Adverse events include life-threatening conditions such as toxic epidermal necrolysis (TEN) and Stevens-Johnson syndrome (SJS), hepatotoxicity, haematological toxicity and gastrointestinal manifestations [4].

ALT = alanine aminotransferase; AST = aspartate aminotransferase; GST = glutathione *S*-transferase; NAT2 = *N*-acetyltransferase 2; PM/DM = polymyositis/dermatomyositis; SLE = systemic lupus erythematosus; SNP = single nucleotide polymorphism; SJS = Stevens-Johnson syndrome; TEN = toxic epidermal necrolysis.

Of the two chemical components of co-trimoxazole, sulphamethoxazole is thought to be responsible for most cases of hypersensitivity [5]. The major metabolic pathway for sulphamethoxazole is catalyzed by *N*-acetylation by *N*-acetyltransferase 2 (NAT2). In the pathogenesis of hypersensitivity, the formation of hydroxylamine through oxidization by cytochrome P450 and its subsequent autooxidation to the nitroso metabolite have been implicated, although these are minor metabolic pathways [6-9]. These toxic metabolites are also detoxified by phase II enzymes and exhibit acetylation by NAT2, glucuronidation by uridine 5'-diphophate-glucronosyltransferase, sulphate conjugation by sulphotransferase, and conjugation with glutathione by glutathione *S*-transferase (GST) [7,10]. Among those metabolizing enzymes, NAT2 is a key enzyme because it catabolizes sulphamethoxazole and toxic metabolites, and may prevent the formation of hydroxylamine.

The *NAT2* gene has at least 13 single nucleotide polymorphisms (SNPs) in the coding exon, and 29 NAT2 alleles (haplotypes) have been described in human populations, as shown in the NAT2 nomenclature Web site [11-13]. In addition to one wild-type haplotype (*NAT2*4*), the human *NAT2* gene has four representative clusters of haplotypes that possess specific nucleotide substitutions at positions 341, 590, 857 and 191. These clusters are called *NAT2*5*, *NAT2*6*, *NAT2*7* and *NAT2*14*, respectively. Previous studies have shown that the members of those clusters are responsible for the slow acetylator phenotype [14,15], which is conveniently determined by examining the concentration of caffeine in urine [16-18]. Individuals who are homozygous for mutant-type haplotypes exhibit the slow acetylator phenotype, whereas those who carry at least one wild-type haplotype exhibit the fast acetylator phenotype.

In the present study we examined the association between genetic polymorphisms in the *NAT2* gene and adverse events with co-trimoxazole in patients with SLE.

Materials and methods

Patients and control individuals

The present study was approved by the Genome Ethics Committee of Tokyo Women's Medical University. A total of 166 patients with SLE were enrolled after they had given informed consent. Of these, 54 were admitted to our hospital between January 2001 and May 2006, and received co-trimoxazole (400 mg sulphamethoxazole and 80 mg trimethoprim) each day for prophylaxis against *Pneumocystis* pneumonia while they were immunosuppressed ($CD4^+$ cell count $<200/mm^3$). All patients with SLE fulfilled the 1997 American College of Rheumatology revised criteria for the classification of SLE [19,20]. The data from these 54 patients were analyzed, and the patients were divided into two groups: those with adverse events ($n = 18$) and those without adverse events ($n = 36$). Among the 18 patients with adverse events, only two experienced severe events that lead to the discontinuation of co-trimoxazole treatment.

We collected samples from three additional patients at two other institutions who experienced severe adverse events. The five patients with severe adverse events (two from our institution and three from the other institutions) were combined to constitute a case group in a case-control study.

We wished to examine whether the genotypes or haplotypes of the *NAT2* gene in SLE patients are different from those in patients with other connective tissue diseases or those from control subject individuals. We therefore obtained genomic DNA from 39 patients with polymyositis/dermatomyositis (PM/DM) who had fulfilled the criteria proposed by Bohan and Peter [21] and from 195 healthy donors (all gave informed consent). All patients and control individuals included in this study were Japanese.

Assessment of adverse events with co-trimoxazole

Liver dysfunction was considered to be present when serum aspartate aminotransferase (AST) or alanine aminotransferase (ALT) levels were higher than twice the upper limit of the normal range. The patients and control individuals had no history of alcohol abuse and were negative for hepatitis B surface antigen and anti-hepatitis C virus antibody. Thrombocytopenia was defined as a platelet count below 100,000/μl. Rashes were variable in severity: TEN was diagnosed when there was widespread epidermal necrolysis with the appearance of scalding (>30% of the body surface area), and epidermal necrolysis that involved less than 10% of the body was diagnosed as SJS.

DNA isolation

On admission to the hospital peripheral blood (10 ml) was drawn from each patient into tubes containing EDTA as an anticoagulant. A standard phenol-chloroform extraction procedure was used to extract genomic DNA from the blood samples.

Genotyping at the single nucleotide polymorphisms in the *NAT2* gene and inference of haplotype combinations

The *NAT2* gene has at least 13 SNPs. Genotyping at four SNP sites enabled us to infer the haplotypes and diplotype configurations for the majority of the Japanese individuals. The four SNP sites included a C to T substitution at nucleotide position 282 (rs1041983), a C to T substitution at nucleotide position 481 (rs1799929), a G to A substitution at nucleotide position 590 (rs1799930) and a G to A substitution at nucleotide position 857 (rs1799931). These four SNPs yield six haplotypes in the *NAT2* gene in the Japanese population, namely *NAT2*4*, *NAT2*5B*, *NAT2*5E*, *NAT2*6A*, *NAT2*7B* and *NAT2*13*. Of these, *NAT2*4* is the wild-type haplotype; the remaining haplotypes are mutant types. In the present study, individuals who were homozygous for mutant-type

haplotypes were tentatively designated slow acetylators; those who carried at least one wild-type haplotype were designated fast acetylators. A predeveloped TaqMan kit (Applied Biosystems, Foster City, CA, USA) that contained a set of forward and reverse primers and fluorescent-labelled probes that hybridize either wild-type or mutant-type sequences was used to determine genotypes at the four SNP sites by allelic discrimination chemistry. Genotypes were determined at four SNP loci in the *NAT2* gene. From the obtained genotype data, we inferred the diplotype configuration for each individual, using PENHAPLO software [22,23]. This program was designed to infer haplotypes for each individual with using the maximum-likelihood method based on the expectation maximization algorithm, assuming Hardy-Weinberg equilibrium for the population [24]. This method infers not only the frequencies of haplotypes in the population but also the distribution of diplotype configurations in each individual.

Statistical analysis

Fisher's exact test was used to evaluate differences in the frequencies of the diplotype configurations corresponding to the slow acetylators (those without *NAT2*4*) between the two groups. Differences were considered to be statistically significant at $P < 0.05$. Relative risks were determined in the cohort study and odds ratios were calculated in the case-control study, with 95% confidence intervals. SAS software (SAS Institute, Cary, NC, USA) was used to compare the differences in ALT levels between two groups using the nonparametric Mann-Whitney U-test.

Results

Haplotypes and diplotype configurations at the *NAT2* gene

Genotyping of the four SNP sites at the *NAT2* gene was sufficient for inferrence of haplotypes or diplotype configurations, using the PENHAPLO program, and the diplotype configuration was concentrated on a single haplotype combination for each individual using this program. Table 1 shows numbers and frequencies of diplotype configurations at the *NAT2* gene in 166 patients with SLE, 39 patients with PM/DM, and 195 healthy individuals. The percentages of fast acetylators were 89.2%, 89.7% and 91.8% among patients with SLE, patients with PM/DM and healthy individuals, respectively (corresponding percentages of slow acetylators were 10.8%, 10.3% and 8.2%). The percentages of fast and slow acetylators were not statistically different between the three groups ($P = 0.66$ by Fisher's exact test).

Incidence of adverse events with co-trimoxazole

The incidence of adverse events was investigated prospectively in 54 patients with SLE who were receiving prophylactic doses of co-trimoxazole. Adverse events occurred in 18 (33.3%) of the 54 patients. Of the 18 patients with SLE who experienced adverse events, two had dual adverse events (yielding a total of 20 adverse events). Of the 20 adverse events, 14 (70%) were liver dysfunction, five (25%) were thrombocytopenia and one (5%) was skin rash. None of fever, gastrointestinal symptom, headache, anaemia, or leucopaenia was observed in the study group.

Table 1

Numbers and frequencies of the diplotype configurations at the *NAT2* gene among patients with SLE, those with PM/DM and healthy individuals

Diplotype configuration	Acetylator phenotype	SLE ($n = 166$)	PM/DM ($n = 39$)	Healthy individuals ($n = 195$)
*NAT2*4/*4*	Fast	84	14	103
*NAT2*4/*5B*	Fast	2	0	0
*NAT2*4/*5E*	Fast	1	0	0
*NAT2*4/*6A*	Fast	43	13	51
*NAT2*4/*7B*	Fast	17	8	24
*NAT2*4/*13*	Fast	1	0	1
Fast acetylators		148 (89.2)	35 (89.7)	179 (91.8)
*NAT2*5B/*5B*	Slow	0	0	1
*NAT2*5B/*6A*	Slow	0	0	2
*NAT2*5B/*7B*	Slow	1	0	0
*NAT2*6A/*6A*	Slow	5	2	6
*NAT2*6A/*7B*	Slow	9	1	6
*NAT2*7B/*7B*	Slow	3	1	1
Slow acetylators		18 (10.8)	4 (10.3)	16 (8.2)

Values are expressed as number (%) of patients. NAT2, *N*-acetyltransferase 2; PM/DM, polymyositis/dermatomyositis; SLE, systemic lupus erythematosus.

Table 2

Association between diplotype configurations at the *NAT2* gene and adverse events with co-trimoxazole, analyzed in the cohort study

Diplotype configuration	Acetylator phenotype	With adverse events ($n = 18$)	Without adverse events ($n = 36$)	Total
*NAT2*4/*4*	Fast	6	15	21
*NAT2*4/*5B*	Fast	0	2	2
*NAT2*4/*5E*	Fast	0	1	1
*NAT2*4/*6A*	Fast	5	12	17
*NAT2*4/*7B*	Fast	2	4	6
Fast acetylators		13 (27.7)	34 (72.3)	47
*NAT2*6A/*6A*	Slow	1	0	1
*NAT2*6A/*7B*	Slow	3	1	4
*NAT2*7B/*7B*	Slow	1	1	2
Slow acetylators		5 (71.4)[a]	2 (28.6)	7

Values are expressed as number (%) of patients. The frequency of adverse events was compared between fast acetylators ($n = 47$) and slow acetylators ($n = 7$). [a]$P = 0.034$ versus fast acetylators (by Fisher's exact test); relative risk = 2.58, 95% confidence interval = 1.34–4.99. NAT2, *N*-acetyltransferase 2.

Association between diplotype configurations at the *NAT2* gene and adverse events with co-trimoxazole

The association between diplotype configurations at the *NAT2* gene and occurrence of adverse events with co-trimoxazole in the cohort study is shown in Table 2. Five out of seven (71.4%) slow acetylators experienced adverse events, and the frequency was significantly higher than that among fast acetylators (13/47 [27.7%]; $P = 0.034$ by Fisher's exact test; relative risk = 2.58, 95% confidence interval = 1.34–4.99). Frequency of immunosuppressant use did not differ between patients who suffered adverse events with co-trimoxazole and those who did not. Thus, concomitant medications did not appear to influence the occurrence of adverse events of co-trimoxazole.

Five patients with severe adverse events were analyzed in a case-control study. Severe adverse events included TEN, SJS, severe liver dysfunction (ALT >300 IU/ml) and severe thrombocytopenia (platelets <50,000/μl), and are summarized in Table 3. As shown in Table 4, three of the five patients with severe adverse events were slow acetylators, and the frequency was compared with that among 52 SLE patients who did not experience severe adverse events (including 16 patients with mild adverse events and 36 patients with no adverse events). The poportion of slow acetylators was significantly higher among the patients with severe adverse events than in those without (60% versus 11.5%; $P = 0.024$ by Fisher's exact test, odds ratio = 11.5, 95% confidence interval = 1.59–73.39).

Influence of diplotype configurations at the *NAT2* gene on serum markers of liver dysfunction

Liver dysfunction as an adverse event can be statistically evaluated using serum markers (ALT and AST). The mean (± standard deviation) interval between the initiation of co-trimoxazole treatment and first observation of liver dysfunction was 15.8 ± 5.2 days. Figure 1 shows serum ALT levels on day 14

Table 3

Clinical characteristics and diplotype configurations at the *NAT2* gene in five patients who experienced severe adverse events with co-trimoxazole

Patient number	Age (years)/sex	Diplotype configuration	Acetylator phenotype	Adverse events
1	52/female	*NAT2*6A/*6A*	Slow	TEN, liver dysfunction
2	56/female	*NAT2*5B/*7B*	Slow	SJS, liver dysfunction
3	43/female	*NAT2*6A/*7B*	Slow	Thrombocytopenia, liver dysfunction
4	48/female	*NAT2*4/*7B*	Fast	Thrombocytopenia
5	46/female	*NAT2*4/*6A*	Fast	SJS, liver dysfunction

NAT2, *N*-acetyltransferase 2; SJS, Stevens-Johnson syndrome; TEN, toxic epidermal necrolysis.

Table 4

Association between diplotype configurations at the *NAT2* gene and severe adverse events with co-trimoxazole, analyzed in the case-control study

Diplotype configuration	With severe adverse events ($n = 5$)	Without severe adverse events ($n = 52$)
Slow acetylator (without *NAT2*4*)	3 (60)[a]	6 (11.5)
Fast acetylator (with *NAT2*4*)	2 (40)	46 (88.5)

Values are expressed as number (%) of patients. The frequency of slow acetylators was compared between five patients who experienced severe adverse events and 52 patients without severe adverse events. [a]$P = 0.024$ by Fisher's exact test; odds ratio = 11.5, 95% confidence interval = 1.59–73.39. NAT2, *N*-acetyltransferase 2.

after initiation of treatment with co-trimoxazole. Levels of serum ALT were significantly higher in slow acetylators than in fast acetylators (median: 82.0 ± 45.3 IU/ml versus 30.0 ± 47.0 IU/ml; $P = 0.0096$ by Mann-Whitney U-test). Serum AST levels immediately after the administration of co-trimoxazole were not significantly different between fast and slow acetylators (median: 30.0 ± 21.5 IU/ml versus 24.0 ± 31.0 IU/ml; $P = 0.088$ by Mann-Whitney U-test). In both groups, baseline levels of serum AST and ALT before administration of co-trimoxazole were within normal limits.

Discussion

The present study demonstrates that, among patients with SLE, slow acetylators (as inferred based on genotype data in the *NAT2* gene) exhibit a greater frequency of various adverse events with co-trimoxazole than do fast acetylators. Ohno and coworkers [14] first reported an association between genetic polymorphisms at the *NAT2* gene and the occurrence of adverse events with sulphonamides. Since then severe adverse events with sulfasalazine, another compound that is catabolized by NAT2, were also reported to be associated with absence of the wild-type allele (*NAT2*4*) in the *NAT2* gene [15,25]. There have been conflicting reports regarding the association between adverse events with co-trimoxazole and *NAT2* genotype, with findings apparently correlating with the underlying disease process. For instance, in the setting of HIV infection many investigators were unable to demonstrate such an association, but some reports have shown a positive association in patients without HIV infection [26]. Therefore, differences in background illness may account for the fact that a positive association was observed in the present study (in patients with SLE) and negative associations were observed in other reports in which the disease was HIV related. An alternative explanation is that there are differences in composition of *NAT2* haplotypes between ethnic groups (as discussed below).

Figure 1

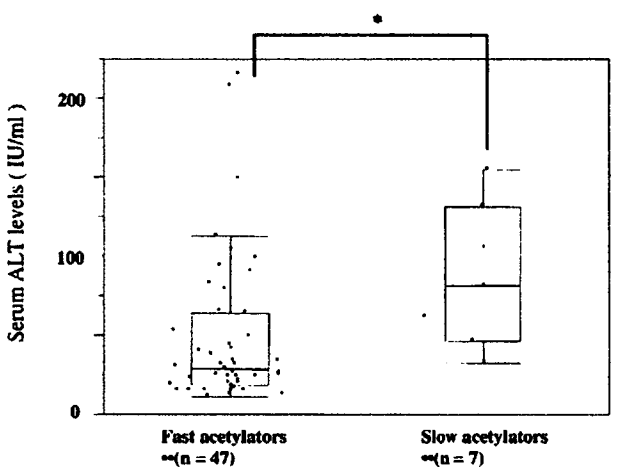

Levels of serum ALT in fast acetylators and slow acetylators. There were 47 fast acetylators and seven slow acetylators in the cohort. Levels of serum ALT in patients with systemic lupus erythematosus were measured 14 day after initiation of co-trimoxazole. Serum ALT levels in slow acetylators were significantly higher than in fast acetylators (median: 82.0 ± 45.3 IU/ml versus 30.0 ± 47.0 IU/ml; *$P = 0.0096$, by Mann-Whitney U-test). ALT, alanine aminotransferase.

In the present study we found that slow acetylators at the *NAT2* gene, among the patients with SLE, were more likely to develop adverse events with co-trimoxazole than were fast acetylators in the cohort study (relative risk = 2.58). In the case-control study, we found that the proportion of slow acetylators was higher among patients with severe adverse events than in those without (60% versus 11.5%; odds ratio = 11.5), although we could not find statistically significant differences between the patients with severe adverse events and 16 patients with mild adverse events (60% versus 25%; $P = 0.28$). We emphasize that severe adverse events, including life-threatening ones, were associated with *NAT2* polymorphisms.

The most frequent adverse event with co-trimoxazole in the cohort study group was liver dysfunction (70%), followed by thrombocytopenia (25%) and rash (5%). The types of adverse events are slightly different from those previously reported for co-trimoxazole. Karpman and Kurzrock [27] reviewed the adverse events associated with co-trimoxazole use in children on full-dose therapy, and indicated that cutaneous lesions were the most common hypersensitivity reactions to co-trimoxazole, accounting for 70% of all adverse events. Other hypersensitivity effects, including fever and haematological toxicity, were also frequent. Liver dysfunction was less common. With sulphonamides, however, liver dysfunction is a well documented common adverse event [28]. We speculate that the incidence of liver dysfunction in patients receiving co-trimoxazole might have been underestimated in the study by Karpman

and Kurzrock [27]. All patients in the present study were hospitalized and monitored for asymptomatic liver dysfunction using routine biochemical tests. Among the 54 patients with SLE who were enrolled in the cohort study, slow acetylators exhibited significantly higher levels of serum ALT after administration of co-trimoxazole than did fast acetylators. This suggests that *NAT2* genotype affected levels of serum ALT. On the other hand, the low incidence of cutaneous lesions in the present cohort study might have been the result of preceding immunosuppressive therapies, latently preventing development of cutaneous lesions.

Sulphonamides are the compounds most associated with development of TEN, and the mechanism of skin necrolysis is reported to be through cytotoxic lymphocyte-mediated pathways and clonally expanded $CD8^+$ T cells [29]. Although TEN and SJS induced by co-trimoxazole is rare, it is a major problem because severe skin disease such as TEN and SJS can occur even with prophylactic doses of co-trimoxazole in SLE. Indeed, some patients in the case-control study exhibited hypersensitivity reactions, including TEN and SJS, which are typical and severe allergic reactions to the drug. Interestingly, a large proportion of these patients were slow acetylators. Thus, polymorphisms at the *NAT2* gene may account even for allergic reactions to co-trimoxazole. These findings are consistent with a previous report [15] demonstrating that allergic reactions such as rashes and fever were more frequent in slow acetylators (as inferred by the maximum-likelihood method) among Japanese patients with rheumatoid arthritis treated with sulphasalazine. The greater frequency of adverse events with co-trimoxazole in slow acetylators might be accounted for by delayed drug clearance, resulting in sustained high levels of serum sulphamethoxazole, which is likely to lead to increased formation of hydroxylamine or nitroso-sulphamethoxazole. These toxic metabolites and sulphamethoxazole might act as cytotoxic, genotoxic, or immunogenic agents, and hence induce adverse reactions.

Haplotype frequencies at the *NAT2* gene vary between ethnic groups. The percentage of slow acetylators was reported to be 56% to 74% among Caucasians [30], but it was only 8.2% in our study. The percentage of slow acetylators in our study is similar to proportions reported previously in the Japanese population [15]. Furthermore, the compositions of mutant haplotypes are quite different between Caucasian and Japanese individuals. In the former, the most frequent mutant haplotype is the *NAT2*5* cluster (45%), followed by the *NAT2*6* cluster (28%) and the *NAT2*7* cluster (2%) [31]. In the Japanese population, however, *NAT2*6A* is the most frequent (20%), followed by *NAT2*7B* (13%), and the *NAT2*5* cluster is very rare (0.01%). Thus, major components of the *NAT2* mutant haplotype in Caucasian individuals are *NAT2*5B* and *NAT2*6A*; in the Japanese population, *NAT2*6A* and *NAT2*7B* are the major components. Each haplotype contains specific nucleotide substitutions: T341C and A803G for *NAT2*5B*, G590A for *NAT2*6A*, and G857A for *NAT2*7B*. All of these substitutions cause amino acid changes. It is curious, however, that the severe adverse events caused by sulfasalazine, associated with *NAT2* variations, have been reported exclusively from Japan, although the frequency of slow acetylators is much higher among Caucasian than Japanese populations [15,25]. The quiet different composition of mutant haplotypes between Caucasian and Japanese populations may account for the difference in adverse events relative to *NAT2* gene haplotype.

During metabolic detoxification of sulphamethoxazole, phase II enzymes other than NAT2 also play a role. GST can detoxify nitroso-sulphamethoxazole by reduction back to hydroxylamine. It catalyzes conjugation of electrophiles with glutathione, thereby inactivating those often cytotoxic or genotoxic substances [32]. Of several GST isozymes, the μ-class enzyme (GSTM), the θ-class enzyme (GSTT) and the π-class enzyme (GSTP) are polymorphic [33-36]. The genetic polymorphisms at the *GSTM1* and *GSTT1* genes were reported to be deletion of nucleotides (referred to as null *GSTM1* and null *GSTT1* alleles), which have been associated with susceptibility to cancer [37,38]. We also investigated the involvement of genetic polymorphisms of the *GSTT1* and *GSTM1* genes in the occurrence of adverse events with co-trimoxazole (data not shown). Nevertheless, none of the *GST* gene polymorphisms were associated with adverse events, a finding that is consistent with previous data [30].

Conclusion

We found that Japanese patients with SLE who do not harbour the *NAT2*4* haplotype develop adverse events with co-trimoxazole more frequently than patients with at least one *NAT2*4* haplotype. Knowledge on diplotype configurations for the *NAT2* gene may lead to improveed efficacy and safety of co-trimoxazole in patients with SLE.

Competing interests

The authors declare that they have no competing interests.

Authors' contributions

MS conceived the study and drafted the manuscript. TS, together with Y Kawaguchi, participated in the design and coordination of the study. MK was responsible for using PENHAPLO software. Y Katsumata, KT, AN, TM and AM recruited a subset of patients. MH recruited a subset of patients and participated in coordination of the study. NK participated in the design and coordination of the study. All authors read and approved the final manuscript.

Acknowledgements

This study was supported by the Research for the Future Program of the Japan Society for the Promotion of Science.

References

1. Bozzette SA, Finkelstein DM, Spector SA, Frame P, Powderly WG, He W, Phillips L, Craven D, van der Horst C, Feinberg J: **A randomized trial of three antipneumocystis agents in patients with advanced human immunodeficiency virus infection. NIAID AIDS Clinical Trials Group.** *N Engl J Med* 1995, **332**:693-699.
2. Hughes WT, Rivera GK, Schell MJ, Thornton D, Lott L: **Successful intermittent chemoprophylaxis for *Pneumocystis carinii* pneumonitis.** *N Engl J Med* 1987, **316**:1627-1632.
3. Ogawa J, Harigai M, Nagasaka K, Nakamura T, Miyasaka N: **Prediction of and prophylaxis against Pneumocystis pneumonia in patients with connective tissue diseases undergoing medium- or high-dose corticosteroid therapy.** *Mod Rheumatol* 2005, **15**:91-96.
4. Straatmann A, Bahia F, Pedral-Sampaio D, Brites C: **A randomized, pilot trial comparing full versus escalating dose regimens for the desensitization of AIDS patients allergic to sulfonamides.** *Braz J Infect Dis* 2002, **6**:276-280.
5. Carr A, Gross AS, Hoskins JM, Penny R, Cooper DA: **Acetylation phenotype and cutaneous hypersensitivity to trimethoprim-sulphamethoxazole in HIV-infected patients.** *AIDS* 1994, **8**:333-337.
6. Rieder MJ, Uetrecht J, Shear NH, Cannon M, Miller M, Spielberg SP: **Diagnosis of sulfonamide hypersensitivity reactions by in-vitro "rechallenge" with hydroxylamine metabolites.** *Ann Intern Med* 1989, **110**:286-289.
7. Cribb AE, Miller M, Leeder JS, Hill J, Spielberg SP: **Reactions of the nitroso and hydroxylamine metabolites of sulfamethoxazole with reduced glutathione. Implications for idiosyncratic toxicity.** *Drug Metab Dispos* 1991, **19**:900-906.
8. Carr A, Tindall B, Penny R, Cooper DA: ***In vitro* cytotoxicity as a marker of hypersensitivity to sulphamethoxazole in patients with HIV.** *Clin Exp Immunol* 1993, **94**:21-25.
9. Gill HJ, Hough SJ, Naisbitt DJ, Maggs JL, Kitteringham NR, Pirmohamed M, Park BK: **The relationship between the disposition and immunogenicity of sulfamethoxazole in the rat.** *J Pharmacol Exp Ther* 1997, **282**:795-801.
10. Cribb AE, Nakamura H, Grant DM, Miller MA, Spielberg SP: **Role of polymorphic and monomorphic human arylamine N-acetyltransferases in determining sulfamethoxazole metabolism.** *Biochem Pharmacol* 1993, **45**:1277-1282.
11. Ilett KF, Kadlubar FF, Minchin RF: **1998 International Meeting on the Arylamine N-Acetyltransferases: synopsis of the workshop on nomenclature, biochemistry, molecular biology, interspecies comparisons, and role in human disease risk.** *Drug Metab Dispos* 1999, **27**:957-959.
12. Hein DW, McQueen CA, Grant DM, Goodfellow GH, Kadlubar FF, Weber WW: **Pharmacogenetics of the arylamine N-acetyltransferases: a symposium in honor of Wendell W. Weber.** *Drug Metab Dispos* 2000, **28**:1425-1432.
13. **Arylamine *N*-acetyltransferase (*NAT*) nomenclature** [http://www.louisville.edu/medschool/pharmacology/NAT.html]
14. Ohno M, Yamaguchi I, Yamamoto I, Fukuda T, Yokota S, Maekura R, Ito M, Yamamoto Y, Ogura T, Maeda K, *et al.*: **Slow N-acetyltransferase 2 genotype affects the incidence of isoniazid and rifampicin-induced hepatotoxicity.** *Int J Tuberc Lung Dis* 2000, **4**:256-261.
15. Tanaka E, Taniguchi A, Urano W, Nakajima H, Matsuda Y, Kitamura Y, Saito M, Yamanaka H, Saito T, Kamatani N: **Adverse effects of sulfasalazine in patients with rheumatoid arthritis are associated with diplotype configuration at the N-acetyltransferase 2 gene.** *J Rheumatol* 2002, **29**:2492-2499.
16. Grant DM, Hughes NC, Janezic SA, Goodfellow GH, Chen HJ, Gaedigk A, Yu VL, Grewal R: **Human acetyltransferase polymorphisms.** *Mutat Res* 1997, **376**:61-70.
17. Grant DM, Tang BK, Kalow W: **A simple test for acetylator phenotype using caffeine.** *Br J Clin Pharmacol* 1984, **17**:459-464.
18. Vatsis KP, Weber WW, Bell DA, Dupret JM, Evans DA, Grant DM, Hein DW, Lin HJ, Meyer UA, Relling MV, *et al.*: **Nomenclature for N-acetyltransferases.** *Pharmacogenetics* 1995, **5**:1-17.
19. Tan EM, Cohen AS, Fries JF, Masi AT, McShane DJ, Rothfield NF, Schaller JG, Talal N, Winchester RJ: **The 1982 revised criteria for the classification of systemic lupus erythematosus.** *Arthritis Rheum* 1982, **25**:1271-1277.
20. Hochberg MC: **Updating the American College of Rheumatology revised criteria for the classification of systemic lupus erythematosus.** *Arthritis Rheum* 1997, **40**:1725.
21. Bohan A, Peter JB: **Polymyositis and dermatomyositis (first of two parts).** *N Engl J Med* 1975, **292**:344-347.
22. Ito T, Inoue E, Kamatani N: **Association test algorithm between a qualitative phenotype and a haplotype or haplotype set using simultaneous estimation of haplotype frequencies, diplotype configurations and diplotype-based penetrances.** *Genetics* 2004, **168**:2339-2348.
23. Furihata S, Ito T, Kamatani N: **Test of association between haplotypes and phenotypes in case-control studies: Examination of validity of the application of an algorithm for samples from cohort or clinical trials to case-control samples using simulated and real data.** *Genetics* 2006, **174**:1505-1516.
24. Kitamura Y, Moriguchi M, Kaneko H, Morisaki H, Morisaki T, Toyama K, Kamatani N: **Determination of probability distribution of diplotype configuration (diplotype distribution) for each subject from genotypic data using the EM algorithm.** *Ann Hum Genet* 2002, **66**:183-193.
25. Ohtani T, Hiroi A, Sakurane M, Furukawa F: **Slow acetylator genotypes as a possible risk factor for infectious mononucleosis-like syndrome induced by salazosulfapyridine.** *Br J Dermatol* 2003, **148**:1035-1039.
26. Zielinska E, Niewiarowski W, Bodalski J, Rebowski G, Skretkowicz J, Mianowska K, Sekulska M: **Genotyping of the arylamine N-acetyltransferase polymorphism in the prediction of idiosyncratic reactions to trimethoprim-sulfamethoxazole in infants.** *Pharm World Sci* 1998, **20**:123-130.
27. Karpman E, Kurzrock EA: **Adverse reactions of nitrofurantoin, trimethoprim and sulfamethoxazole in children.** *J Urol* 2004, **172**:448-453.
28. Pullar T: **Adverse effects of sulphasalazine.** *Adverse Drug React Toxicol Rev* 1992, **11**:93-109.
29. Chave TA, Mortimer NJ, Sladden MJ, Hall AP, Hutchinson PE: **Toxic epidermal necrolysis: current evidence, practical management and future directions.** *Br J Dermatol* 2005, **153**:241-253.
30. Pirmohamed M, Alfirevic A, Vilar J, Stalford A, Wilkins EG, Sim E, Park BK: **Association analysis of drug metabolizing enzyme gene polymorphisms in HIV-positive patients with co-trimoxazole hypersensitivity.** *Pharmacogenetics* 2000, **10**:705-713.
31. Srivastava DS, Mittal RD: **Genetic polymorphism of the N-acetyltransferase 2 gene, and susceptibility to prostate cancer: a pilot study in north Indian population.** *BMC Urol* 2005, **5**:12.
32. Mannervik B, Danielson UH: **Glutathione transferases: structure and catalytic activity.** *CRC Crit Rev Biochem* 1988, **23**:283-337.
33. Seidegard J, Pero RW, Miller DG, Beattie EJ: **A glutathione transferase in human leukocytes as a marker for the susceptibility to lung cancer.** *Carcinogenesis* 1986, **7**:751-753.
34. Pemble S, Schroeder KR, Spencer SR, Meyer DJ, Hallier E, Bolt HM, Ketterer B, Taylor JB: **Human glutathione S-transferase theta (GSTT1): cDNA cloning and the characterization of a genetic polymorphism.** *Biochem J* 1994, **300**:271-276.
35. Arand M, Muhlbauer R, Hengstler J, Jager E, Fuchs J, Winkler L, Oesch F: **A multiplex polymerase chain reaction protocol for the simultaneous analysis of the glutathione S-transferase GSTM1 and GSTT1 polymorphisms.** *Anal Biochem* 1996, **236**:184-186.
36. Nakajima T, Elovaara E, Anttila S, Hirvonen A, Camus AM, Hayes JD, Ketterer B, Vainio H: **Expression and polymorphism of glutathione S-transferase in human lungs: risk factors in smoking-related lung cancer.** *Carcinogenesis* 1995, **16**:707-711.
37. Dalhoff K, Buus Jensen K, Enghusen Poulsen H: **Cancer and molecular biomarkers of phase 2.** *Methods Enzymol* 2005, **400**:618-627.
38. Chan EC, Lam SY, Fu KH, Kwong YL: **Polymorphisms of the GSTM1, GSTP1, MPO, XRCC1, and NQO1 genes in Chinese patients with non-small cell lung cancers: relationship with aberrant promoter methylation of the CDKN2A and RARB genes.** *Cancer Genet Cytogenet* 2005, **162**:10-20.

Journal of Clinical Apheresis 22:323–329 (2007)

Recruitment of Immature Neutrophils in Peripheral Blood Following Leukocytapheresis Therapy for Rheumatoid Arthritis

Masako Okawa-Takatsuji,[1]* Katsuya Nagatani,[1] Kyoichi Nakajima,[2] Kenji Itoh,[2] Toshikazu Kano,[2] Chiaki Nagashio,[2] Yuko Takahashi,[2] Shinichi Aotsuka,[1] and Akio Mimori[2]

[1]Department of Community Health and Medicine, Research Institute, International Medical Center of Japan, Tokyo, Japan
[2]Division of Rheumatic Diseases, International Medical Center of Japan, Tokyo, Japan

The objective of this study is to evaluate the cellular mechanism underlying filtration leukocytapheresis (LCAP) therapy for the treatment of rheumatoid arthritis (RA). Thirteen patients with refractory RA each underwent three sessions of LCAP. Before (pre-) and after (post-) the completion of the first LCAP session, peripheral blood was sampled and analyzed for neutrophil surface markers using flow cytometry. The surface antigens of peripheral blood mononuclear cells (PBMCs) and neutrophils obtained at pre- and post-LCAP were then analyzed using a fluorescence-activated cell sorter. The American College of Rheumatology's criterion of a 20% improvement was achieved in six patients, but not in the other seven patients, after LCAP therapy. The post-LCAP number of blood band-form neutrophils with a bone marrow phenotype ($CD49d^{dim+}$, low density) was higher among the responders than among the nonresponders, suggesting an association between the clinical response and the recruitment of bone-marrow-derived neutrophils. After the nonspecific absorption of WBCs during a 1-h Cellsorba procedure, the number of PBMCs was consistently decreased, although the number of neutrophils that were affected by removal plus recruitment varied in a manner that was independent of efficacy. In contrast, the emergence of immature neutrophils in the peripheral blood was characteristic of the effective therapies. These cells were found after the 1st session of responders and also found following sessions of LCAPs. Immature neutrophils, which may be recruited from the bone marrow in the peripheral blood after the first session of LCAP, can predict the clinical efficacy of subsequent LCAP sessions. J. Clin. Apheresis 22:323–329, 2007.

Key words: LCAP; band-formed neutrophils; CD49d; FACS

INTRODUCTION

Rheumatoid arthritis (RA) is a chronic inflammatory disease that often results in joint destruction; effective therapeutic strategies for RA include the inhibition of DNA synthesis in activated immunocompetent cells and the blockade of proinflammatory cytokines [1]. Leukocytapheresis (LCAP) may provide an additional measure of therapeutic efficacy in patients with refractory RA when combined with conventional therapy. An LCAP adsorption column composed of fine polyester fibers [2] has been developed to eliminate possibly pathogenic leukocytes from the circulating blood of patients with RA or ulcerative colitis (UC) [3,4]. In fact, an improvement in RA symptoms after LCAP with minimal adverse effects has been confirmed by clinical studies [3–8], including randomized controlled trials in patients with UC [7] or RA [8]; sham apheresis was used as a placebo control in the latter study.

In contrast to its established clinical efficacy, the mechanisms of action underlying LCAP therapy are not fully understood. In an early study, LCAP reduced the activated monocyte counts in the peripheral blood of RA patients after repeated LCAP [9]. A later study suggested a reduction in the number of activated CD4+ T cells in the synovial fluid of RA patients after LCAP [10], while another study demonstrated an elevation in serum interleukin (IL)-10 levels in RA patients after repeated LCAP, but no changes in the serum levels of tumor necrosis factor-α, IL-1, IL-2, IL-6, IL-8, or IL-15 [11].

As in the previous study, we found that the level of IL-10 in the serum of post-LCAP patients was significantly elevated. The induction of cells that produce, if any, antiinflammatory cytokine IL-10 may be a beneficial action of LCAP, although the administration of ex-

*Correspondence to: Masako Okawa-Takatsuji, PhD, Department of Community Health and Medicine, Research Institute, International Medical Center of Japan, 1-21-1 Toyama, Shinjuku, Tokyo 162-8655, Japan. E-mail: okawat@ri.imcj.go.jp

Received 6 August 2007; Accepted 27 November 2007

Published online 19 December 2007 in Wiley InterScience (www.interscience.wiley.com).
DOI: 10.1002/jca.20155

ogenous IL-10 might not be an effective strategy for treating RA [12].

A study on granulocyte–monocyte-apheresis for the treatment of patients with UC reported a reduction in IL-8 mRNA expression in the colonic mucosa of patients after therapy [13], and this procedure was also found to be effective for the treatment of patients with RA [14]. Columns packed with cellulose acetate beads were used in these studies, and these columns effectively adsorbed blood granulocytes and monocytes, but not lymphocytes [15].

The use of LCAP with a polyester–fiber-column eliminates close to 100% of neutrophils and monocytes and a majority of lymphocytes from the blood that is passed through the column; a large number of neutrophils, but not monocytes or lymphocytes, are immediately recruited into the peripheral blood [5,16].

In the present study, we investigated the change in cellular compositions before and after the LCAP session, especially in regard to recruited neutrophils containing stab-formed immature-neutrophils. We found that neutrophils measured after the first session served as an indicator of the efficacy of LCAP therapy.

PATIENTS AND METHODS

Patients

Thirteen patients with active RA (10 women and 3 men) were treated using LCAP. Their mean age was 65.1 ± 12.5 years (range, 35–83 years), and their mean disease duration was 8.3 ± 8.3 years (0.3–28 years). RA was diagnosed according to the American College of Rheumatology (ACR) criteria [17]. The Ethics Committee of the International Medical Center of Japan approved the present study, and all the patients gave their written informed consent. All the patients were treated with prednisolone (5–10 mg/day) plus at least one antirheumatic drug, methotrexate or leflunomide, except for two patients in whom both antirheumatic drugs had been discontinued because of side effects. Only one patient was treated with an anticytokine biological agent.

LCAP Procedure

LCAP was performed three times at 1-week intervals in each patient. During each session, 3,000 mL of venous blood was extracorporeally circulated through a Cellsorba adsorption column composed of fine polyester fibers (Asahi Kasei Medical Co., Tokyo, Japan) at a flow rate of 50 mL/min for 60 min using nafamostat mesilate (50 mg/h) for anticoagulation, according to the standard procedure.

Clinical Evaluation of the Patients

Before the first LCAP session and 1 week after the final LCAP session, the disease activity was evaluated according to the ACR core set [18]. Patients who showed an improvement in the ACR criteria of 20% or more were classified as responders.

Blood Sampling

Immediately before (pre-LCAP) and 10 min after the completion (post-LCAP) of the first LCAP session in all the patients, peripheral venous blood was sampled and used to perform a circulating leukocyte count, a serum cytokine assay, and a flow cytometric leukocyte analysis. In some patients, blood was also sampled after another LCAP session. The serum was frozen and stored for later analysis. Blood for the flow cytometry analysis was drawn using a heparinized syringe and mixed with one-fifth the volume of 6% dextran in PBS and incubated for 15 min at 37°C. The upper leukocyte-rich fraction of the blood was obtained, diluted twice with saline, and centrifuged with Ficoll-Hypaque (SG 1.077) at 400*g* for 20 min. The mononuclear cell fraction on the Ficoll interface was obtained and washed three times with Hank's balanced salt solution containing 0.2% EDTA, then resuspended in PBS containing 2% FCS (2% FCS-PBS) for fluorescence-activated cell sorter (FACS) staining.

Flow Cytometry

The mononuclear cell fraction on the Ficoll interface were stained for cell-surface markers with FITC- or PE-conjugated monoclonal antibodies to CD3, CD19, CD14, CD11b, and CD49d (BD Biosciences, CA), or FITC- or PE-conjugated mouse IgG1 as an isotype control (BD Biosciences). After incubation with the antibodies on ice for 30 min, the cells were washed with 2% FCS-PBS. After washing, the stained cells were analyzed using a FACSCalibur Flow Cytometric System (Becton Dickinson, NJ).

Enzyme-Linked Immunosorbent Assay

Paired pre- and post-LCAP sera from the first session were assayed for IL-10 and granulocyte-colony stimulating factor (G-CSF) using an IL-10 enzyme-linked immunosorbent assay (ELISA) kit and a human G-CSF ELISA kit, respectively (BioSource Int., CA).

Statistical Analysis

The data were expressed as the mean ± SD and were statistically analyzed using the *t*-test and the paired *t*-test. Differences with $P < 0.05$ were considered significant.

RESULTS

Clinical Evaluation of LCAP Therapy

Disease activity in the 13 patients was evaluated before the first LCAP session (baseline) and at 1 week after the completion of three sessions of LCAP (after